Mon. Not. R. astr. Soc. (1985) **217**, 601–631

The high-redshift evolution of radio galaxies and quasars

J. A. Peacock *Royal Observatory, Blackford Hill, Edinburgh EH9 3HJ*

Accepted 1985 July 4. Received 1985 July 3; in original form 1985 April 24

Summary. This paper presents a new investigation into the evolution with cosmological epoch of the luminosity function for extragalactic radio sources. The free-form technique of Peacock & Gull has been applied to an increased data base of complete samples and number counts, with improved statistical methods, resulting in an important reduction of the uncertainties in the derived luminosity functions.

For the class of compact flat-spectrum sources, the present data require a redshift cut-off, with the luminosity function ceasing to evolve at $z \simeq 2$ and being reduced at $z=4$ by a factor of $\gtrsim 3$ from its peak value. For the radio-source population as a whole, however, no such statement can yet be made. Experiments to resolve this uncertainty are discussed; the implication is that surveys only a factor ~ 10 deeper than existing complete samples will contain substantial fractions of high-redshift objects (~ 20 per cent $z>3$), *unless* the above redshift limit is a general one.

The physical implications of a redshift cut-off are discussed. The possibility of obscuration at high redshift which is a source of uncertainty for optically selected quasars does not affect radio-based studies. It seems likely that the formation of radio galaxies took place relatively recently in cosmological terms.

1 Introduction

Radio astronomy and cosmology have been closely connected since the first identifications of bright radio sources with objects at high redshift. Early hopes of using these cosmological probes to find H_0 and q_0 were not fulfilled, but the study of the cosmological history of the radio-source population nevertheless retains a great deal of interest. The aim, as with studies of optically selected quasars, is to learn from the statistical population evolution something about the history of individual sources. In particular, one of the outstanding questions relates to the existence of a hypothetical epoch of formation, a limiting redshift beyond which no objects exist. To date, this long-predicted feature of the early Universe has not definitely been observed, although there has been some controversy over its possible appearance in optical quasar searches (Osmer 1983; Koo 1983). One of the main objectives of this paper is to study the uncertainties in our present

knowledge of events at high redshift from the radio view-point, and to guide the planning of future observations to improve that knowledge.

The main justification for using radio-selected samples is in terms of completeness: at high galactic latitudes, simple flux-density-limited surveys contain only extragalactic objects. The selection effects are thus much more readily quantifiable than when a dominant galactic contamination has to be removed. Further, radio sources (although not their optical counterparts) are largely immune to the effects which can complicate studies of objects at high redshifts: e.g. dust obscuration (Ostriker & Heisler 1984) or gravitational lensing (Peacock 1982). This simplicity is bought at the price of incomplete redshift information, however. The problem which must be solved is thus to find the limits allowed by incomplete data to the comoving density of sources as a function of source luminosity (P) and redshift (z): the Radio Luminosity Function (RLF) $\varrho(P,z)$ (note that we will always define ϱ as the number per unit $\log_{10} P$). The present paper is an improvement and extension of an earlier analysis of this sort by Peacock & Gull (1981; PG). Incorporation of new data and more powerful statistical techniques has allowed considerable refinement of PG's conclusions. Section 2 discusses the general approach adopted and results are given in Section 4. Section 3 summarizes practical details of the method and data used, technical details being given in Appendices 1 and 2. Finally, the important conclusions of this study are discussed in Sections 5 and 6.

2 Modelling luminosity functions

The technique used in this paper is model fitting – the search for a set of analytic luminosity functions which are in statistical agreement with all existing data. As this method has been subject to criticism, it seems worthwhile to begin with a discussion of the advantages of this approach to the problem.

Deduction of the luminosity function for a given population of objects is straightforward in principle, but is complicated by finite sampling volumes and incomplete data. The ideal situation would be a survey complete over the whole sky to an arbitrarily low flux density, with a redshift for every source; the luminosity function could then be constructed by simple binning in a range of luminosity and distance. The result is of course a function of the bin size used, and ceases to be useful for bins so small as to contain only one object. This is a natural limit which causes problems when we come to interpret the luminosity function and its dependence on epoch. For example, one ultimate aim would be to construct a picture involving the physics of individual sources via the conservation equation:

$$\frac{\partial \varrho}{\partial t}+\frac{\partial}{\partial L}(\dot{L}\varrho)=Q, \tag{2.1}$$

where $\dot{L}$ is the rate of change of $\log(P)$ for a source of luminosity P, and Q is the rate of creation of objects at that luminosity. However, this equation cannot be applied directly as we cannot take the limit to find the derivatives of ϱ. Formally, we must instead assume that the objects we observe are the result of some grand experiment consisting of independent random drawings from a density function ϱ, which might satisfy equation (2.1). The question then becomes one of how much we can deduce about ϱ from the limited data. The forward problem is easier than the inverse: statistical tests can decide whether a given analytical guess for ϱ could have been the function from which the data were drawn. Since we can clearly deduce nothing about the small-scale (in P and z) variations of ϱ, it is sensible to restrict attention to functions which vary only on scales which our data can probe. This is not to say that our Universe must have been drawn from such a function, only that we can never distinguish it from a smoothed version of itself.

Considerations of this sort have motivated the various attempts to model the RLF – i.e. to find a parameterized analytic guess for ϱ which is fitted to the observed data. Previous work in this field was surveyed by PG; the most important recent papers were due to Wall, Pearson & Longair (1980, 1981; WPL I and WPL II). This approach is rendered most valuable by incompleteness in redshift information, for the redshift content of surveys is poorly defined except at high flux densities. Although the RLF is thus unknown in regions of the P–z plane corresponding to low flux densities, a consistent model is of value because it extrapolates the trends observed in the region where the RLF is well defined. Moreover, the extrapolation is constrained by the partial information on the unknown region (source counts and identification statistics: see Appendix 2). In practice, this extrapolation is most simply achieved by PG's technique of series expansion:

$$\log\varrho=\sum_{i=0}^{n}\sum_{j=0}^{n-i}A_{ij}x^i(P)y^j(z), \tag{2.2}$$

where x and y are transformed axes of the P–z plane, and the series is truncated at the lowest expansion order consistent with the data. However, what we need is a measure of the *uncertainty* in this extrapolation; in practice 30–40 unknown A_{ij} parameters must be specified to fit the data, and we should be most unwise to trust the extrapolation of such a highly tuned function (although note that 10–12 of these parameters specify only the local RLF, which other workers give numerically). What we must do, therefore, is consider an ensemble of different model RLFs, formulated in different ways. Where the problem is ill-constrained, the various extrapolations will in general differ; we can aid this divergence by assuming various values for unknown data items and attempting to fit them. Thus the work in this paper considers five rather different model RLFs in the hope that they will span approximately the uncertainty in smooth extrapolations of existing data. There can be no guarantee that the complete range of uncertainty has been mapped. Where the model RLFs differ, we may be certain our data are inadequate; where they agree, on the other hand, there is always the possibility that the agreement is fortuitous and not required by the data. There are two ways of proceeding: one is to construct a test of the existing data to investigate directly the aspect of interest suggested by the modelling results (Section 4.4 adopts this approach with respect to evolution at high redshift). Alternatively, we can accept the model results as a working hypothesis, and proceed to make falsifiable predictions for the outcome of future cosmological experiments, in a manner analogous to that of a genuine physical theory. The main aim of the present work, then, is to examine the range of predictions for faint samples allowed by new models of the RLF produced on the above hypothesis of smoothness. By finding where these extrapolations are well-constrained, we can optimize the design of future experiments to probe particular features of the RLF. Specifically, we can determine the best way of searching for the redshift cut-off – this is the subject of Section 5.

3 Construction of the RLFs

At this stage, we need to specify how a trial luminosity function is to be compared to the data and discuss which datasets to use. These matters were discussed by PG and so have been relegated to appendices here: Appendix 1 considers model-building techniques and Appendix 2 the data. In the main, the methods and data used are similar to PG; the most essential features are:

(i) The model RLFs are dual-population, with a division based on high-frequency radio spectral index α: steep-spectrum ($\alpha\geq0.5$) and flat-spectrum ($\alpha<0.5$). This aspect is unchanged from PG.

(ii) The PG data base has been augmented by inclusion of new complete samples, of which the most important is a sample of 41 flat-spectrum sources with $S_{2.7}>0.5$ Jy.

The major difference between PG and this work is in the techniques for obtaining a model RLF that fits the data, which we now discuss.

3.1 GOODNESS OF FIT AND RLF OPTIMIZATION

The data sets described in Appendix 2 are of two distinct types: the bright complete samples where we have the observable (S, z) for every source, and the binned results from published source counts, etc. Binned data are usually compared with a model via the χ^2 test; while binning is to be avoided in principle, the data are often not published in any other form. When the number of objects per bin is large (as is usually the case) then the loss of statistical power in using χ^2 to test goodness of fit is not important.

Conversely, the bright complete samples are restricted in size, and it is crucial to use efficient statistical techniques to extract all the information contained in these data sets, which were obtained only at expense of much observational effort. In this case we wish to compare the empirical distribution of points over the S–z plane with the distribution expected for a given RLF.

The comparison of this density law with the empirical distribution of data points may be carried out using a two-dimensional version of the Kolmogorov–Smirnov (KS) test described by Peacock (1983). This is efficient in that it uses each data point individually by comparing empirical and hypothetical cumulative distributions across the S–z plane. Note that the procedure used by PG (and all other RLF modellers) was grossly inefficient by comparison with this: they only tested the fit to the source counts and luminosity distributions separately, using binned data and a χ^2 criterion. In our present terms, only the marginal distributions $dN(S)$ and $dN(z)$ were constrained, taking no account of correlations on the S–z plane (which are certainly present – see Wall & Peacock 1985). Thus, it is no surprise in retrospect that PG found that the correct values of $\langle V/V_{\max}\rangle$ were not reproduced by their initial RLFs and had to be added as an extra constraint. The 2-D KS procedure, conversely, uses all the data in the bright-source samples and consistent values of $\langle V/V_{\max}\rangle$ are guaranteed when the constraining is done in this way. Note that analyses such as WPL I and II and more recently that by Condon (1984), which use only source counts and redshift distributions, can in contrast produce RLFs inconsistent with the complete-sample S–z data.

We now need to combine the goodness-of-fit measures for individual data sets into a single figure of merit to assess the fit of a given RLF as a whole. Probably the most formally correct way of achieving this is in terms of the significance levels p_i, i.e. the probability that the misfit statistic for the ith data set would be larger than the observed value by chance. The null hypothesis for independent data sets is that the p_is should be uniformly distributed between 0 and 1; this could be tested by the normal KS statistic. There are, however, several problems with this: (i) the data sets are not strictly independent, since surveys at different frequencies count the same sources several times; (ii) the KS test is inefficient at detecting a few values of p_i close to zero; (iii) the null hypothesis is modified by the fact that our whole procedure is designed to manipulate $\varrho(P, z)$ so that the p_i are maximized in some sense. The last point is probably not important since the number of undetermined parameters used to express ϱ is considerably less than the number of degrees of freedom in the data (in any case, as the problem is non-linear we cannot say that estimating n parameters from the data reduces the number of degrees of freedom by n – there is no guarantee that any non-negative ϱ could fit the data precisely). The first two points tell us that we would be wise not to worry about the precise distribution of the p_i, but to form instead a statistic which would be efficient at detecting too many low values for some of the p_i. One straightforward way of achieving this is via

$$W \equiv \prod_{i=1}^{n} p_i. \tag{3.1}$$

On the null hypothesis, the distribution of $\ln W$ for large n will be normal, with mean n and variance n. This statistic detects low values of p_i in a direct and satisfactory way, and does not place strong emphasis on the distribution of p_is close to 1.

While W is a convenient measure of goodness of fit over several diverse data sets, it turns out not to be suitable for use in the scheme to optimize the RLF. Any iterative scheme to maximize W would involve solving

$$\mathbf{H}\cdot\delta\mathbf{A}=-\mathbf{G}, \tag{3.2}$$

where $\mathbf{A}$ is a vector of the parameters describing the RLF, $\mathbf{G}$ is the vector of first derivatives of W with respect to the A_i and $\mathbf{H}$ is the Hessian matrix of second derivatives (see PG). Now, for statistics of the KS type, the point of maximum misfit can change discontinuously as the theoretical distribution is altered, which leads to discontinuities in $\mathbf{G}$. In short, the p_i from the K–S tests do not vary sufficiently smoothly with RLF expansion parameter for a second-order search to be possible.

An alternative method commonly used to optimize models is that of maximum likelihood. This can be applied here with no difficulty since, for the binned data, the likelihood L is

$$L\propto\exp(-\chi^2/2), \tag{3.3}$$

and for a sample with complete (P, z) data

$$L\propto\prod_{i=1}^{N}\frac{\varrho(P_i, z_i)}{\langle N\rangle} \tag{3.4}$$

where $\langle N\rangle$ is the predicted size of the sample.

If we could be confident of the correctness of one particular expansion for ϱ, then maximizing $L_{\rm tot}$ would be a rigorously correct approach; as it is, a given expansion can only be judged by the *a posteriori* goodness-of-fit tests discussed above. A maximum-likelihood method has two disadvantages: (i) the value of χ^2 in (3.3) is summed over all data sets. This last point means that a minimum $-\chi^2$ solution could occur in which all the high residuals were grouped unacceptably in one data set – a problem encountered by PG. These difficulties may be circumvented by combining the W-statistic and ML methods as follows: first evaluate W for all data sets apart from the ones where the KS test would be applied. The distribution of W may be specified in terms of

$$\chi^2_W=\frac{(\ln W-M)^2}{M}, \tag{3.5}$$

where M is the number of data sets involved. We may now define a new likelihood for all data sets:

$$L_{\rm T}=L_{\rm c}\exp(-\chi^2_W/2) \tag{3.6}$$

where $L_{\rm c}$ is the likelihood for the complete (S, z) samples – equation (3.4). Minimizing $L_{\rm T}$ gives us a solution which is more satisfactory in that it uses our knowledge of the partition of the binned results into different data sets. The final result may be tested by computing the total W-statistic over all data. As with all ML solutions, the value of W is not guaranteed to be acceptable – this would indicate some defect in the formulation of the model. In practice, the modified-ML method above did achieve solutions which were globally acceptable, without the unsatisfactory necessity of adding weight to poorly fitted data sets, as PG were forced to do.

3.2 CHOICE OF COSMOLOGY

Any uncertainty in the RLF is compounded by our ignorance of the large-scale geometry of the Universe, i.e. the dependence on redshift of luminosity distance and comoving volume. Most workers have assumed a model (invariably Friedmann with various values of q_0), derived ϱ, and repeated the analysis for various cosmologies (e.g. PG used $q_0=0$ and 0.5). In fact, this repetition is not necessary, as may be seen from (A1.5). The LHS of this equation is observable and independent of geometry, so that the RLFs for two different geometries, ϱ_1 and ϱ_2, are related by

$$\varrho_1(P_1,z)\frac{dV_1}{dz}=\varrho_2(P_2,z)\frac{dV_2}{dz}, \tag{3.7}$$

where P_1 and P_2 are the luminosities derived from (S,z) via (A1.1). The only complication to this is the variation of spectral index with P: we have

$$P_1/P_2=D_1^2/D_2^2 \tag{3.8}$$

which is a function of redshift. The assumption $\alpha=\alpha(P_1)$ thus implies $\alpha=\alpha(P_2,z)$ in the new geometry. Since α depends only slowly on $\log P$, this redshift effect will be unimportant unless P_2/P_1 becomes several orders of magnitude. The fundamental geometry adopted here is Friedmann with $q_0=0.5$, and α correlated with P only for steep-spectrum sources. For values of z and q_0 of interest, $0.5\leqslant P_1/P_2\leqslant 2$ and the error in α, introduced if the $P-\alpha$ relation in fact applies for a different q_0, is negligible. We can thus simply deduce the effect on ϱ of different geometries; only variations in q_0 will be examined here, but more radical alternatives could be considered just as easily.

3.3 THE RLF ENSEMBLE

As in PG, a range of differently formulated model RLFs which are consistent with the data have been derived, and uncertainties in the RLF will be estimated by considering the differences between the various models. Consistent in this case means that the final goodness of fit over all data sets was acceptable at about 1 per cent level; the variations between the model RLFs thus give a lower bound to the 99 per cent confidence limits on $\varrho(P,z)$. The fundamental model is number 1: the (P,z) coordinates used for expansion are $(\log P,z)$, and integration is terminated at $z=10$. The expansion orders are fifth order (21 terms) for the steep-spectrum RLF (plus one extra term in $(\log P)^6$ to assist in fitting the sharp kink in the local RLF) and fourth order (15 terms) for the flat-spectrum RLF. The other models vary successively one aspect of this as follows:

RLF 2 adds an exponential cut-off at high P as suggested by Wall & Peacock (1985): $\varrho\propto\exp(-P/P_c)$ with $P_c=10^{28}\,\mathrm{W\,Hz^{-1}\,sr^{-1}}$ was taken.

RLF 3 uses a redshift coordinate of $\log_{10}(1+z)$ instead of z.

RLF 4 integrates only out to $z=5$.

RLF 5 assumes that the local RLF also gives the low-P end of $\varrho(P,z)$ at $z=0.4$ (*cf.* models 1–4 which assume no evolution to $z=0.2$ only).

These modifications (limits in P and z, enforcement of zero evolution for low luminosity) assume some extreme possibilities for the situation in poorly constrained areas of the $P-z$ plane, in an attempt to explore the full range of possibilities allowed by the data. In what follows, we assume that this objective has been achieved, and that any feature seen in all models is probably real. As emphasized in Section 2, the next step is always to construct an experiment to test this hypothesis. To indicate the goodness of fit achieved, Figs 1 and 2 compare data and range of predictions for various source counts and the local RLF.

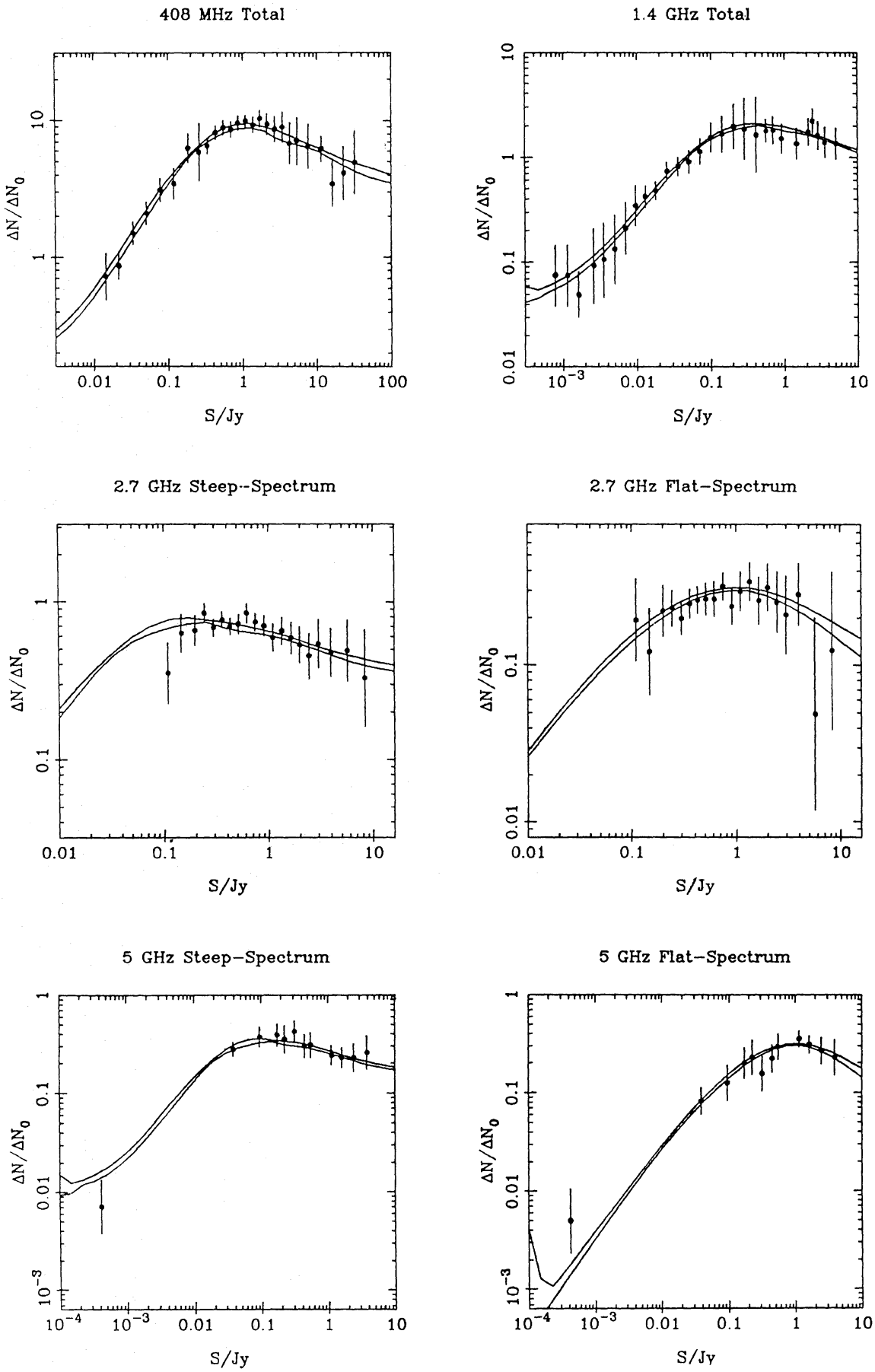

Figure 1. The data on differential source counts [normalized to $N_0=100\,(S/\mathrm{Jy})^{-1.5}\,\mathrm{sr}^{-1}$] and the limits on $\Delta N/\Delta N_0$ from the RLFs described in Section 3. The error bars plotted are $\pm 2\sigma$.

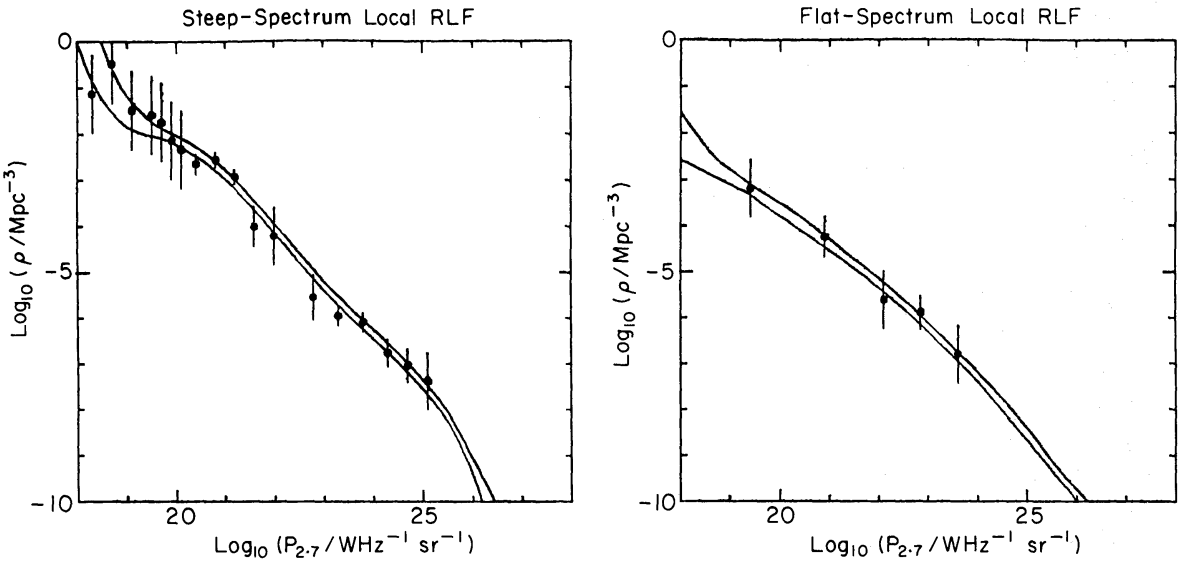

Figure 2. The data on the local RLF, together with the limits on ϱ_0 from the RLFs described in Section 3. The error bars plotted are $\pm 2\sigma$.

The expansion parameters for the various RLFs are given in Appendix 3. A density parameter $\Omega=1$ is assumed in the models above but translation to other values of Ω is straightforward (see above).

4 Results

4.1 UNCERTAINTY MAPS

To see which areas of the P, z plane are well constrained, we follow PG and consider R, the ratio of the smallest to the largest value of ϱ found at a given gridpoint, considering all model RLFs. Fig. 3 shows contours of R (to be compared with PG, fig. 7); lines showing the loci of constant flux densities of 1 Jy and 1 mJy at 2.7 GHz are also plotted. The improvement in these diagrams is not at high flux densities, where the statistics are fundamentally limited, but faintwards of 1 Jy. The

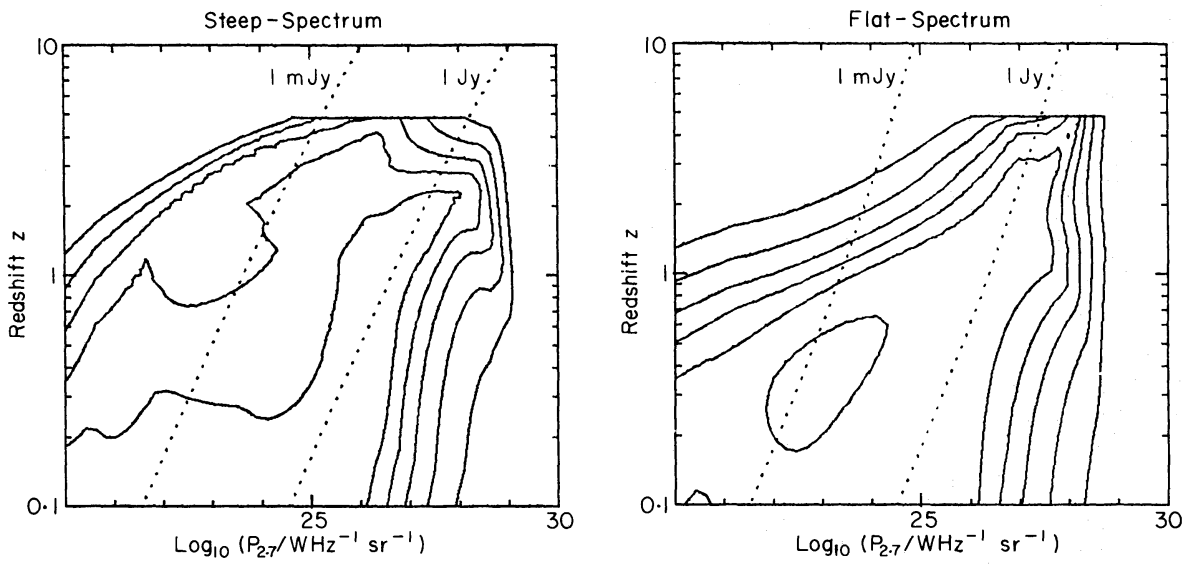

Figure 3. Contours of the reliability $R \equiv (\varrho_{MIN}/\varrho_{MAX})$ over the P–z plane for $q_0=0.5$. Contours are at $\log_{10} R = -0.2$, -0.5, -1, -2, -4.

RLF appears now to be well determined out to $z \simeq 0.5$ for all $P \lesssim 10^{26}\,\mathrm{W\,Hz^{-1}\,sr^{-1}}$. This has been achieved by a combination of the improved statistics at high flux density giving a more constrained extrapolation to lower flux densities, together with the new identification statistics and the fact of no evolution for $z<0.2$. Interestingly, the forcing of no evolution out to $z=0.4$ for low luminosities in model 5 appears not to change ϱ greatly at that redshift with respect to the models which are free to evolve, confirming immediately the near-constancy of ϱ at low luminosities.

The behaviour at high redshift is well known only in a region closer to the 1-Jy line – in the approximate luminosity range 10^{25}–$10^{27}\,\mathrm{W\,Hz^{-1}\,sr^{-1}}$. This particular region is the subject of Section 4.3.

4.2 RATES OF EVOLUTION

The most important of PG's conclusions concerned the relation between the strengths of evolution for steep- and flat-spectrum sources. In contrast with previous authors, PG proposed that all data on flat-spectrum sources could be understood if both spectral classes underwent differential evolution, with similar strength for the most powerful sources of either type. We now wish to re-examine this proposal in the light of the new results.

Some confusion exists on this topic through the frequent emphasis on the results of $V/V_{\max}$ analyses. Although this statistic is a convenient indicator of evolution, it is not an estimator for the rate of change of ϱ. Empirically, it is useful to define a variable m related to the time derivative of ϱ via

$$m(P,z)=\frac{\partial\{\ln\varrho(P,z)\}}{\partial\tau} \tag{4.1}$$

where, as usual, τ is look-back time in units of the age of the Universe {i.e. $\tau=1-(1+z)^{-1}$ ($q_0=0$) or $1-(1+z)^{-1.5}$ ($q_0=\frac{1}{2}$)}. This simplifies comparison with early assumed forms of quasar evolution laws which held m constant. Fig. 4 shows limits on $m(P)$ over the redshift range 0.3–1 (neglecting high and low redshifts where the evolution is not well determined). The values of $m(P)$ are not strictly differential but are derived from the total change in ϱ over this redshift

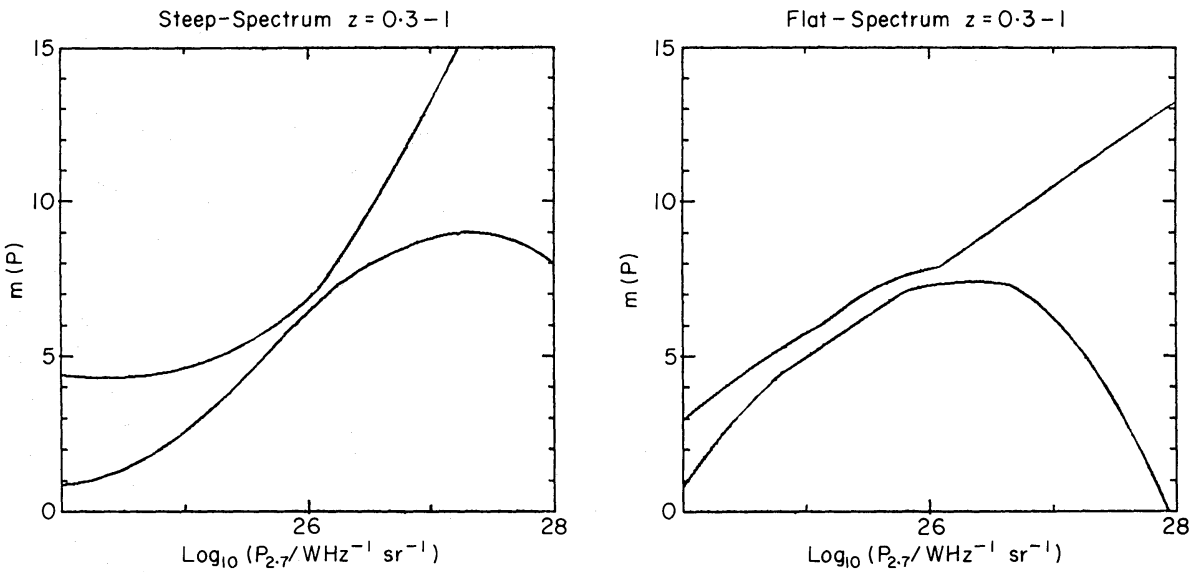

Figure 4. The limits to the strength of evolution $m(P, z)$ in the redshift range $z=0.3$–1 allowed by the RLFs of Section 3.

range, as determined from the various model RLFs. However, the assumption of constant m over these redshifts is a good one (*cf.* Fig. 5). The interesting feature of these diagrams is the similarity between the behaviour of flat- and steep-spectrum sources: $m(P)$ is only significantly positive for $P \gtrsim 10^{24}\,\mathrm{W\,Hz^{-1}\,sr^{-1}}$, and increases with power, reaching $m=8$–10 at the highest powers. There may be some suggestion that the flat-spectrum $m(P)$ is higher at $P \sim 10^{26}\,\mathrm{W\,Hz^{-1}\,sr^{-1}}$, but this is only a marginal effect. These diagrams are the updated basis for the well-established statement that the radio-source population evolves differentially, i.e. faster for higher powers. This conclusion has been criticized by Condon (1984), who states that differential evolution is not required, but he is using the term in a different sense from the normal one. Condon's point was that he could construct a consistent RLF which underwent a combination of density and luminosity evolution:

$$\varrho(P,z)=g(z)\varrho\{P/f(z)\}. \tag{4.2}$$

As neither f nor g depended on power, Condon concluded that luminosity-dependent evolution was not required. This is a play on words, however: because the local RLF is strongly curved (e.g. Wall & Peacock 1985), the effect of $f(z)$ is to change ϱ by a larger amount at high power – differential evolution in the usual sense. Condon's conclusion would be important if evolution of the RLF were related directly to evolutionary tracks of individual sources, but, because the lifetimes of objects are so short, the dominant effect is probably the unknown birth function (Q in equation 2.1): it is not clear what the physical meaning of (4.2) might be.

The above results are similar to those of PG, who produced RLFs with negative evolution for low luminosity, which was criticized as a severe defect by Swarup, Subrahmanya & Kapahi (1982). In fact, negative evolution is not *required*: the limits on $m(P)$ for low P are very broad and we have already argued in Section 4.1 that $\varrho(z=0.4)$ and $\varrho(z=0)$ need not differ at all at low P. Further, it is important to establish that such behaviour is allowed, despite preconceptions, as it could have a physical basis: if the strong evolution of the RLF were attributed to the dimming of the powerful sources only, then we would indeed expect the low-luminosity end of the RLF to increase with decreasing redshift (albeit by a small amount). It may be noted that analysis of the Leiden–Berkeley deep survey data by Windhorst (1984) led to the conclusion that mild positive evolution did exist for luminosities around the break in the local RLF ($P_{2.7} \sim 10^{23}\,\mathrm{W\,Hz^{-1}\,sr^{-1}}$). The reason for this stronger conclusion is that the result depends on the detailed interpretation of redshifts estimated from galaxy photometry, whereas we have made more conservative use of the data here (see Appendix 2), being more concerned with evolution at higher luminosities.

As to the relative values of $m(P)$ for steep- and flat-spectrum sources, does this finally settle the controversy as to which class evolves fastest? The answer must remain no, as the situation is frequency-dependent. If 1-GHz luminosities were used instead, the flat-spectrum $m(P)$ would be the higher, because of the dependence of m on P and the different spectral indices of the two populations. It may be that the question is not meaningful, given the existence of differential evolution.

4.3 BEHAVIOUR AT HIGH REDSHIFT

In studying the evolution of the RLF at high redshifts, there is a problem of presentation. As discussed in Section 4.1, the RLF is well known at high z only over a restricted luminosity range, so that plotting the RLF at a variety of redshifts would give a confused impression. A simpler alternative is to study cuts at constant luminosity in the well-defined region.

Fig. 5 shows the limits on ϱ for a variety of luminosities and values of q_0 (for the different geometries, ϱ has been translated in luminosity and scaled by the ratio of volume elements as

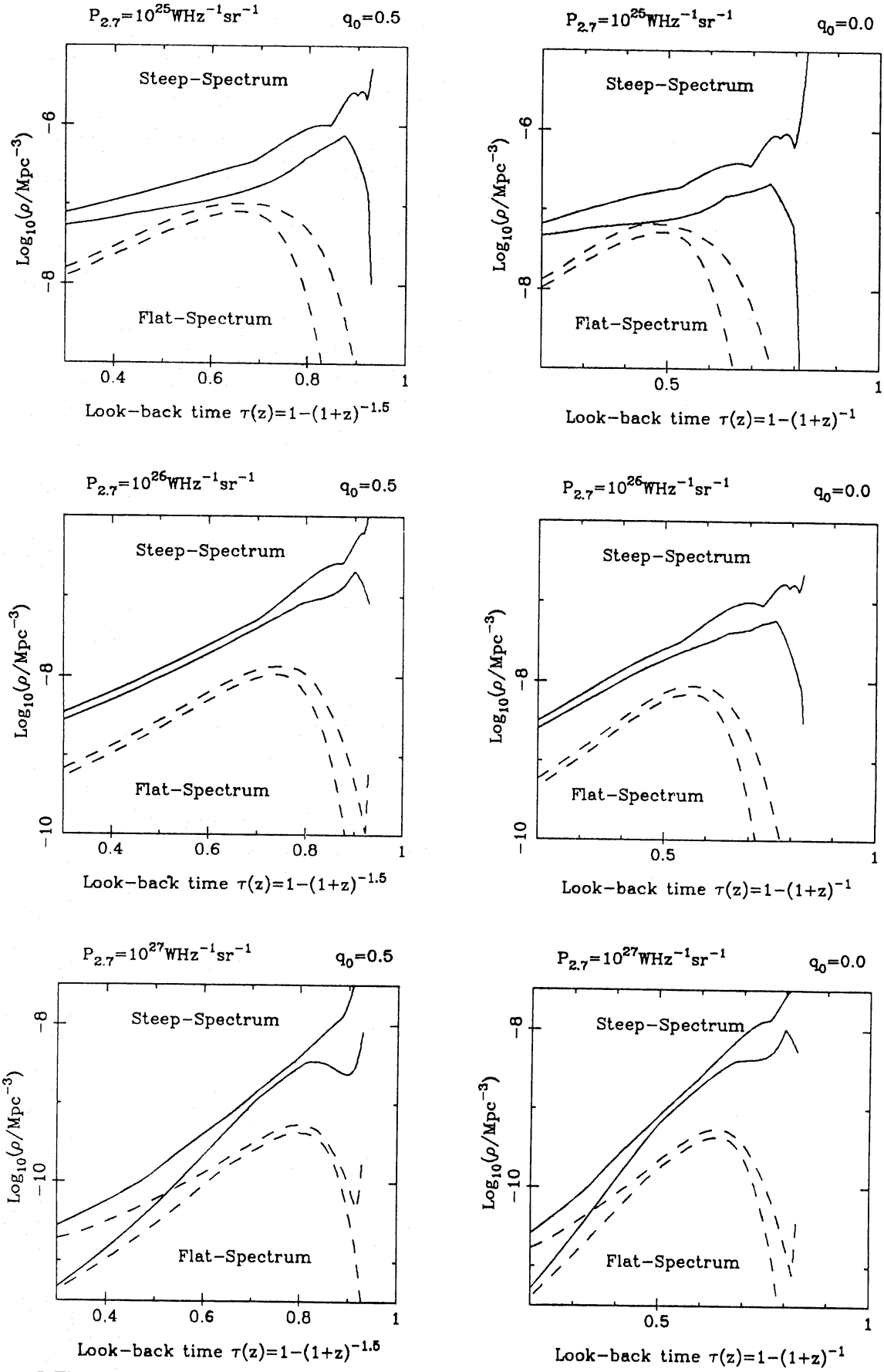

Figure 5. The limits to ϱ at constant P allowed by the RLFs of Section 3, plotted against look-back time normalized to the age of the Universe, τ. Note (i) the behaviour close to $\varrho \propto \exp(m\tau)$ for $z \sim 1$; (ii) the reduction of ϱ beyond $z \simeq 2$ for flat-spectrum sources (shown dashed).

discussed above). The redshift scale has been chosen as normalized look-back time τ, for the ease of comparison with the previous section.

The remarkable feature of these diagrams is that, independent of luminosity or geometry, the comoving density at high redshifts falls for flat-spectrum sources. For the steep-spectrum population, the uncertainties are larger: we cannot distinguish between the same drop as the flat-spectrum sources, or continuing evolution. What is of particular interest is the critical redshift involved in the turnover. The maximum density occurs at a redshift of about 2 and is lower at $z=4$ by a factor of 2–4. This would imply that the decade-old suspicion of a redshift limit at $z\simeq2.5$ has turned out to be essentially correct, despite the subsequent appearance of quasars with $z>3$ to prove that the cut-off could not be abrupt.

The most important question raised by the above result is what data set is causing the turnover. It would be unsatisfactory if such a feature appeared in all consistent RLF models without a more direct explanation being possible. Accordingly, in the next section the complete-sample data are analysed with especial emphasis on evolution at $z\gtrsim2$. What emerges is that the above result is directly due to the lack of quasars with $z>2.5$ in the 0.5-Jy sample, and further that this could have been deduced from the data in Wills & Lynds (1978) alone.

4.4 DIRECT INVESTIGATION OF HIGH-REDSHIFT EVOLUTION

The purpose of this section is to re-examine in a model-independent way the evolution of the flat-spectrum population. We wish to see to what extent the redshift limit discussed above can be deduced from the complete-sample data alone, and to study the sensitivity of this result to factors such as use of estimated redshifts.

Fig. 6 shows the fundamental data available in the form of plots of luminosity against flux density. This makes clear the requirements for a successful probe of high-redshift space. With only two complete steep-spectrum samples available, only a narrow range of flux density is sampled at a given luminosity and we cannot distinguish between a redshift limit and a cut-off in luminosity at the upper end of the RLF. What is required is many high-luminosity sources at high flux density, which should appear with $z\gtrsim4$ at lower flux densities, provided the space density of such objects has not fallen. This condition is satisfied for the flat-spectrum samples because of the

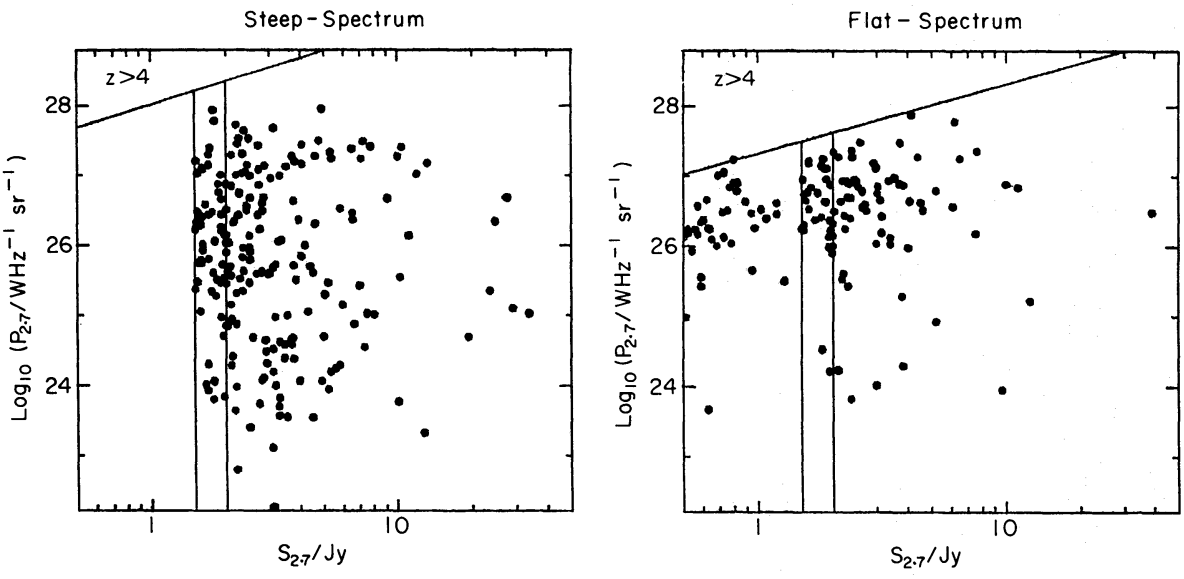

Figure 6. The redshift data for the complete samples used here, plotted on the $P(q_0=0.5)$–S plane. The lines indicate flux-density limits at 1.5 and 2 Jy and the area of the P–S plane in which objects with $z>4$ would lie.

extension of the flux-density limit to 0.5 Jy: this deep sample contains almost no objects with $P_{2.7}>10^{27}$ W Hz^{-1} sr^{-1}. In short, we know of high-luminosity objects with $z\sim1$, which should be easily detectable at $z\sim4$ at lower flux density but which are not found. The best way of quantifying this sort of statement is to use the coherent V_e/V_a statistic of Avni & Bahcall (1980), which is a generalization of the classical V/V_{max} test. This procedure allows us to combine several different samples with different flux-density limits by considering the total volume defined by the survey depth as a function of area on the sky. For example, a bright source at low redshift might in principle have appeared instead at high redshift in a faint sample: it thus has a large volume *available* to it. If all such luminous sources were found only at low redshift, the volume *enclosed* by them would be small and a deficit of distant objects would be indicated if $\langle V_e/V_a\rangle<0.5$. This is still not quite what we require, however, because the strong positive evolution for $z\lesssim2$ masks any possible downturn at higher redshift. To study high redshifts only, we can use a further modification of the test to work in redshift bands (Osmer & Smith 1980; Avni & Schiller 1983). Restricting attention to redshifts $>z_0$, with corresponding cosmological volume V_0, the hypothesis of uniform RLF implies that

$$\left\langle\frac{V_e-V_0}{V_a-V_0}\right\rangle=0.5 \tag{4.3}$$

to within the statistical rms uncertainty, $(12N)^{-1/2}$ for N objects. Table 1 shows the results of this banded V_e/V_a calculation. Some care is necessary here because of the presence of sources with

Table 1. $\langle V_e/V_a\rangle$ for the flat-spectrum samples. (i) All sources; (ii) sources with measured redshifts only; (iii) random perturbation of estimated redshifts.

i)

		$\langle V_e/V_a\rangle$	
redshift range	n	$q_o = 1/2$	$q_o = 0$
>1.8	26	0.370	0.422
>1.9	24	0.315	0.352
>2.0	16	0.356	0.403
1.9 - 3.25	23	0.359	0.376

ii)

		$\langle V_e/V_a\rangle$	
redshift range	n	$q_o = 1/2$	$q_o = 0$
>1.8	14	0.336	0.380
>1.9	12	0.319	0.362
>2.0	10	0.278	0.324
1.9 - 3.25	12	0.433	0.446

iii)

	$\langle V_e/V_a\rangle$	
redshift range	$q_o = 1/2$	$q_o = 0$
>1.8	0.425 ± 0.03	0.475 ± 0.03
>1.9	0.413 ± 0.03	0.465 ± 0.03
>2.0	0.382 ± 0.03	0.439 ± 0.03
1.9 - 3.25	0.480 ± 0.03	0.496 ± 0.03

estimated redshifts. The normal $V/V_{\max}$ test is insensitive to these, depending largely on how close a given source is to the flux-density limit of the sample. Where a redshift band is considered, it is important whether the estimated redshifts lie at the top or bottom of the band. The calculation has therefore been performed in three ways: (i) using the redshifts best-guessed from apparent magnitude; (ii) considering only those objects with spectroscopic redshifts (or an estimate in the case of definite galaxy identifications); (iii) changing the estimated redshifts in a series of Monte Carlo trials. In this last case, the assigned redshifts were altered by a random factor distributed between -0.2 and 0.2 in $\log_{10} z$, corresponding to a magnitude error of ± 1 mag (in this case, the mean and rms variation in the results of the trials are given). The result from calculations (i) and (ii) are in close agreement: for z_0 in the range 1.8–2.0, $\langle V_e/V_a \rangle$ is in the range 0.3–0.4, indicating a significant deficit of high-redshift flat-spectrum sources. The values in the third case are higher, typically by 0.1, but still always less than 0.5. These higher values arise because the objects with estimated redshifts are presently predicted to lie at similar redshifts to those with spectroscopy; introducing a scatter allows a significant number at higher redshifts. In short, the present calculations indicate a deficit of sources at high redshift; unless many of the objects without spectroscopy turn out to have $z>3$, the result seems secure. Observations to test this possibility are clearly important.

Savage & Peterson (1983) have suggested a mechanism that could produce an apparent deficit of flat-spectrum sources at high redshift. It is supposed that all radio spectra become optically thin at high frequency, then flat-spectrum sources taken to high enough redshift would change their classification to steep-spectrum. This argument can be investigated directly. If we parameterize spectral curvature via a parameter β such that

$$\beta = \frac{d\alpha}{d \log_{10} \nu}, \tag{4.4}$$

then a limiting redshift z_L is defined by

$$\log_{10}\{(1+z_L)/(1+z)\} = (\alpha - 0.5)/\beta. \tag{4.5}$$

Beyond z_L, the source is classified as steep-spectrum. Typical values of β are ~ 1, but repetition of the V_e/V_a analysis with $\beta=3$ and $z_{\max}$ not allowed to exceed z_L again fails to alter the values in Table 1 significantly. We conclude that spectral curvature is not causing an apparent deficit of high-redshift flat-spectrum objects.

This lack of high-redshift sources is surprising when compared with results for optically selected quasars. The motivation for Osmer (1983) to search for quasars at $z \simeq 4$ was that Osmer & Smith (1980) had apparently established that quasar evolution continued to $z>3$ without any cut-off. More exactly, they found that $\langle V_e/V_a \rangle$ over the redshift band 1.9–3.25 was 0.61 ± 0.08, very different from our result. In fact, two of the values of $V/V_{\max}$ in the Osmer & Smith paper are incorrect: their result should have been 0.595. Osmer & Smith took $q_0=0$; for $q_0=0.5$ the result is 0.651, in complete disagreement with Table 1. This need not mean that one of the values is in error, as the Osmer & Smith result applies for quasars of the highest optical luminosity ($M_B \simeq -30$). Koo (1983) has reported work which indicates that, for low optical luminosities, the comoving density falls for $z \gtrsim 2$, whereas for higher luminosities this is not so. The significance of this result lies in the optical luminosities of radio-selected quasars, which typically have $M_B \simeq -26$. Hence, both radio and optically selected studies are in agreement that the comoving density falls for $z \gtrsim 2$, with the exception of the most extreme optically luminous quasars. A possible explanation of this difference is provided by gravitational lensing: the optical luminosity function is so steep at the brightest end $\{N(>L_0) \sim L_0^{-3}\}$, that selection effects may be dominant at high redshift. Peacock (1982) showed that observed samples could be heavily increased in size by

magnification of intrinsically faint objects, if the luminosity function was steep enough. The optical function is sufficiently steeper than the RLF (for which $N(>P)\sim P^{-2.5}$: see Wall & Peacock 1985) that this may well explain the discrepancy. This possibility will be investigated in more detail elsewhere.

Finally, we note that this disagreement between optically selected and flat-spectrum radio quasars could have been discovered earlier. Many of the 0.5-Jy quasars are in the samples of Wills & Lynds (1978). Evaluating the same $\langle V_e/V_a\rangle$ as above for their flat-spectrum $\pm 4°$ quasars yields 0.326 ± 0.09 (11 objects) – with $z=1.9$–3.25, $q_0=0.5$ – in good agreement with our result, despite the lack of the bright comparison samples.

The agreement of the flat-spectrum radio results with those of Koo (1983) for low-L_0 quasars gives confidence that the decline in comoving density for $z\gtrsim 2$ is correct and thus suggests that it may apply to the steep-spectrum radio population also. Strategies for studying this possibility are considered in the next section.

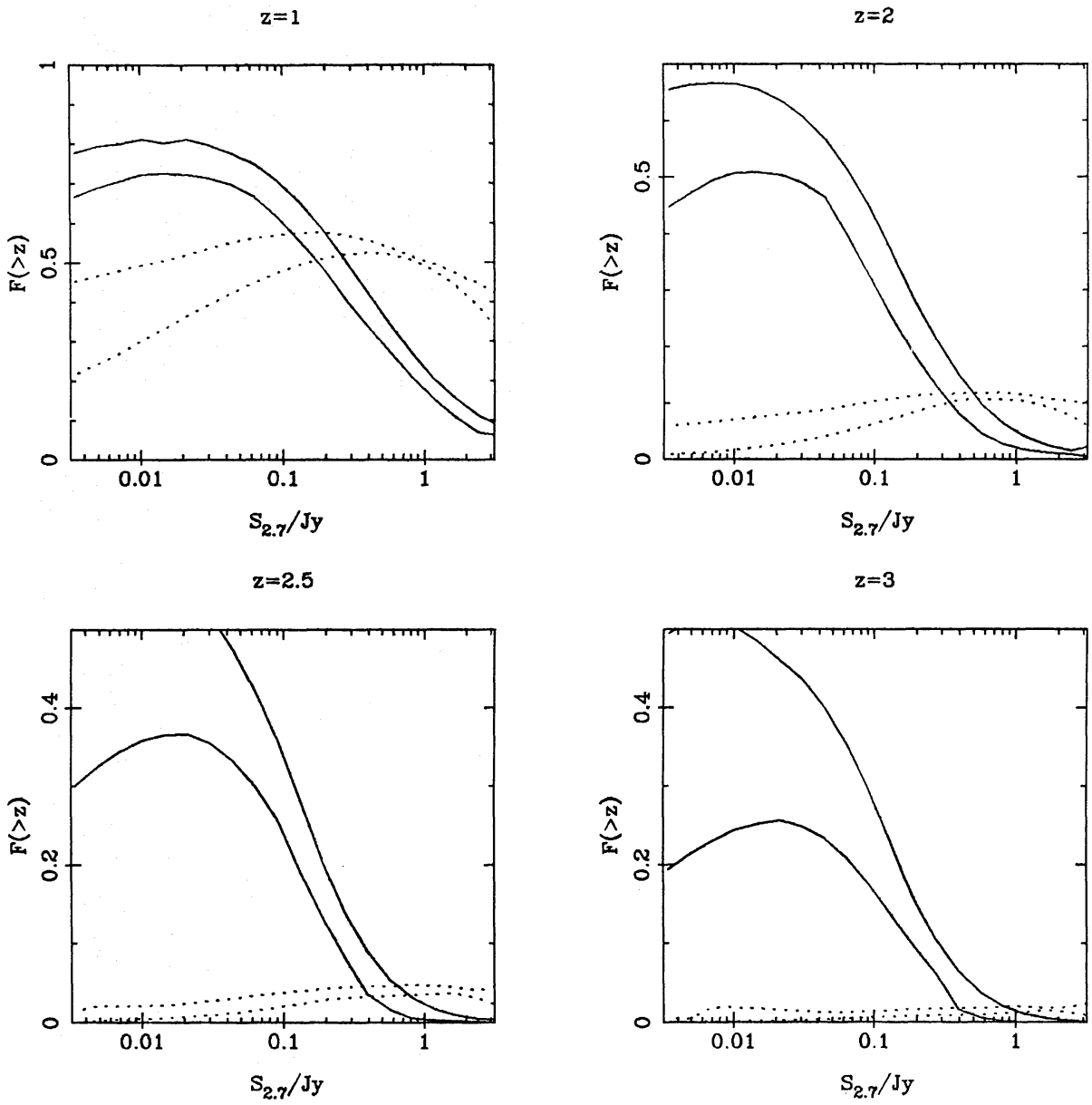

Figure 7. The fractions $F(>z)$ predicted for steep-spectrum (full lines) and flat-spectrum (dotted lines) sources as a function of limiting flux density, for various redshifts.

5 Observational predictions

Constraints on the behaviour of the RLF at high redshift are most simply obtained by having a fainter complete sample to compare with those already available. We can get an idea of how faint we need to go by examining the model predictions for the redshift content of deeper surveys. Fig. 7 shows the limits to the fraction $F(>z)$ for various redshifts as a function of limiting flux density, for each spectral type individually. For flat-spectrum sources, these fractions are small above $z=2$ ($\lesssim$5 per cent) – as expected from the discussion in the previous section. Conversely, the lack of unambiguous convergence in the steep-spectrum RLFs at high redshift allows these fractions to become substantial – with perhaps 50 per cent of steep-spectrum sources having $z>2$ at a flux-density limit of $S_{2.7}\simeq 100$ mJy, only a factor 10–15 deeper than the complete samples used here. To examine this spectacular increase in numbers of high-redshift objects more closely, Fig. 8 shows the redshift distributions predicted for a sample limited at $S_{2.7}=0.1$ Jy, in cumulative form. For steep-spectrum sources (which constitute about 70 per cent of all objects at this level), the predictions agree well up to $z\simeq 1$, beyond which there is a great divergence of opinion. In the most extreme case, fully 20 per cent of the sources have $z\gtrsim 5$; this is no doubt unrealistic, but the whole point of the present work is to establish that such possibilities *cannot* be ruled out. At the opposite extreme, we have the RLFs which exhibit a turnover in Fig. 5, although even these have 10–15 per cent of the steep-spectrum population lying at $z>3$. The observational situation is thus clear: unless optical work at these radio levels reveals a very substantial number of high-redshift objects, then we will be forced to conclude that the radio-source population as a whole follows the flat-spectrum minority in having a space density reduced beyond a redshift of about 2. The Parkes Selected Region surveys, with a limit of $S_{2.7}=0.1$ Jy, are ideally suited for this experiment; optical work to test the above predictions is in progress (Downes *et al.* 1985).

Again, it is instructive to see if the above predictions can be obtained more directly from the complete-sample data. Suppose we knew the density law $\varrho(z)$ which was appropriate for the luminous objects in the bright-source samples. We could then form the density-weighted volume

$$V'(z)=\int \varrho(z)dV(z). \tag{5.1}$$

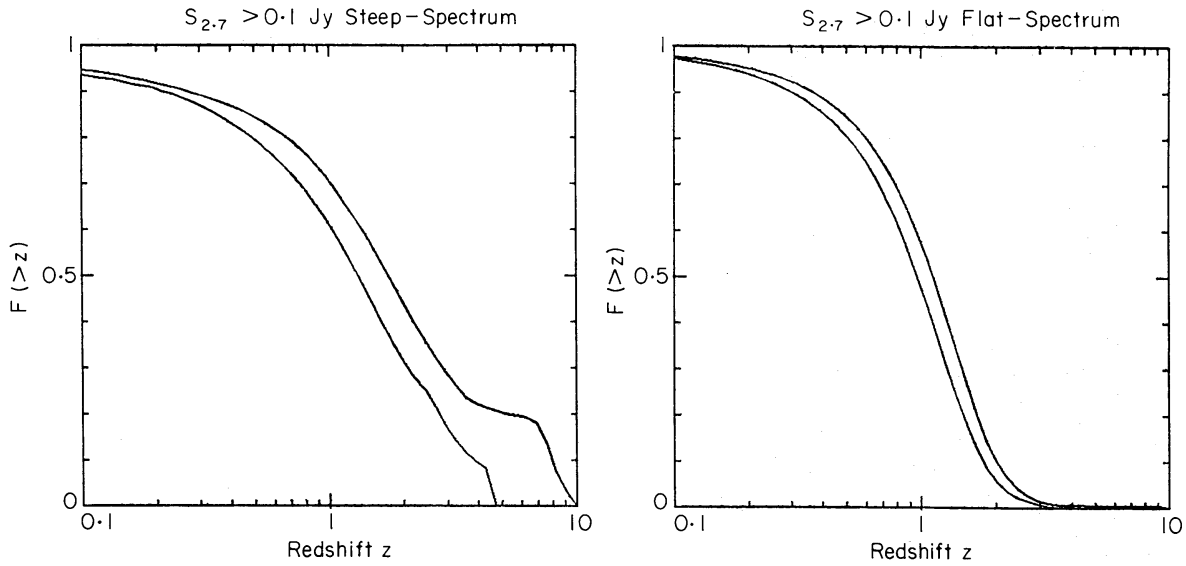

Figure 8. The cumulative redshift distributions of steep- and flat-spectrum sources predicted for the Parkes Selected Regions (178 sources in 0.0753 sr with $S_{2.7}>100$ mJy).

As discussed by Avni & Bahcall (1980), an acceptable form for $\varrho(z)$ would yield $\langle V'_e/V'_a\rangle$ close to 0.5. In terms of this new volume, the maximum-likelihood estimator for the density ϱ' is

$$\varrho' = \sum \frac{1}{V'_a}, \tag{5.2}$$

where the summation is over the objects in the complete samples. The expected number of sources in a new survey can thus be estimated by finding the volume V' in the new sample within which any of the known objects could have been detected and multiplying by ϱ'. This prediction was carried out using two alternative density laws:

(i) $\varrho \propto \exp(10\tau)$ $z<2$
ϱ constant $z>2$
(ii) $\varrho \propto \exp(10\tau)$ all z,

where τ is look-back time as defined in Section 5.3 and $q_0=0.5$ was taken (use of $q_0=0$ produces similar results). Using only the sources in the 1.5- and 2-Jy samples with $P_{2.7}>10^{25}\,\mathrm{W\,Hz^{-1}\,sr^{-1}}$, we can first predict the numbers of high-redshift ($z>2$) sources expected in the 0.5-Jy flat-spectrum sample: the forms (i) and (ii) predict respectively 19 and 35 sources with $z>2$. As the true number is between 5 and 22 depending on the unknown redshifts, we already have strong evidence against continuing strong evolution at $z>2$. Extension of these predictions to the selected regions (178 sources in 0.0753 sr with $S_{2.7}>0.1$ Jy) is even more impressive: the predicted numbers of steep-spectrum sources with $z>2$ on the two hypotheses are 24 and 37 as against 66 and 123 flat-spectrum. The latter figures exceed the total flat-spectrum count at that level – illustrating how source counts can provide useful constraints even in the complete absence of redshift data. The direct figures for the steep-spectrum sources confirm the model RLF results: even with no evolution at $z>2$, ~20 per cent of the steep-spectrum sources at the 100 mJy level should lie at $z>2$.

Lastly, we should mention the possibility of carrying out similar analyses to constrain the high-redshift RLF at lower powers. Windhorst (1984) attempts to use the Leiden–Berkeley deep survey (see Appendix 2) for this purpose, with the conclusion that, for $P_{2.7}\lesssim 10^{24}\,\mathrm{W\,Hz^{-1}\,sr^{-1}}$, the RLF must fall beyond $z\simeq 1$. This is clearly very important if true, but at this stage the result cannot be regarded as conclusive for the following reasons. First, it considers radio galaxies only; some 20 per cent of existing identifications are quasar candidates, which could well make up any high-redshift deficit in the total RLF. Secondly, the result is largely based on photometric redshift estimation; spectra exist for ≤15 per cent of the sample. Thirdly, the modelling technique used extrapolates the low-redshift RLF, taking no account of uncertainty in the low-redshift behaviour. The extrapolation is especially worrying, as there are no measured redshifts >0.6. This contrasts with the present work where many sources are known directly to lie in the critical range $z\simeq 1.5$–2.5. In short, further work is needed before the existence of a redshift cut-off in the RLF at low powers can be established.

6 Discussion

This paper has produced evidence that there may be a decrease in the comoving density of powerful radio sources at high redshift, with the RLF falling by a factor ≳3 over the redshift range 2–4. We have considered experiments to verify this assertion; if the redshift limit fails to hold in general, then surveys at intermediate flux-density levels must contain substantial fractions of very high redshift objects. Assuming for now the correctness of this picture, we wish to see to what extent the result can be reconciled with current ideas for galaxy formation.

The first point to consider is the possibility of an optical illusion: can obscuration prevent us seeing objects at $z \gtrsim 3$? The main process which might affect centimetre-wavelength radio emission is Thomson scattering due to an ionized intergalactic medium. The resulting optical depth as a function of redshift is given by Longair & Rees (1973) (apart from a misprint):

$$\tau = 0.02 \left(\frac{H_0}{50} \right) \frac{\Omega_{\rm IGM}}{\Omega^2} \{(1+\Omega z)^{1/2}(3\Omega+\Omega z-2)+2-3\Omega\}. \quad (6.1)$$

Even making the unrealistically favourable assumption of $\Omega_{\rm IGM} \simeq \Omega = 1$, we only attain $\tau = 0.2$ at $z = 4$; for a steep luminosity function, $\varrho \propto P^{-\gamma}$ with $\gamma = 2$–2.5, this produces a change of about 0.2 in $\log_{10} \varrho$. This is much smaller than the effect we seek, especially as the reduction in $\log_{10} \varrho$ between $z = 2$ and 4 is only half of this. In the optical, things are more interesting: obscuration by dust (discussed most recently by Ostriker & Heisler 1984) could plausibly become important at high redshifts. Ostriker & Heisler consider only $\Omega = 1$, but in general, for dust with opacity proportional to λ^{-1}, the mean optical depth is:

$$\tau = \tau^* \int \frac{(1+z)^2}{(1+\Omega z)^{1/2}} dz. \quad (6.2)$$

Ostriker & Heisler consider that plausible values for τ^* may lie in the range ~ 0.1–1 (B band). Even for $\tau^* = 0.1$, the values of τ at $z = 2.5$ and 4 are (0.9, 2.2) for $\Omega = 1$ and (1.4, 4.1) for $\Omega = 0$: certainly large enough to suppress *optical* counterparts severely at high redshift. The best candidates for objects which have suffered this fate are very red faint optical identifications. For example, the source 0202+14 (one of the members of the 2.7-GHz All-Sky Sample of Wall & Peacock 1985) was identified with an object having $r = 21.9$ on a deep CCD exposure by Peacock *et al.* (1981). Subsequently, Rieke, Lebofsky & Wisniewski (1982) showed the object to be extremely red, with $r - K \simeq 6$. This is much greater than usually found for quasars, and would be more characteristic of a radio galaxy at $z > 1$ (Lilly & Longair 1984). However, the radio source is compact and flat-spectrum and Rieke *et al.* (1982) find variability in the infrared, suggesting that it is a quasar. Clearly, spectroscopy of this and similar objects will be invaluable in testing the hypothesis of dust obscuration. Nevertheless, it seems unlikely that dust can cause an illusory turn-down in the distribution of high-redshift radio sources. For this to occur, the 0.5-Jy flat-spectrum sample would have to contain many objects at $z = 3$–4 which have been obscured (see Section 5); in fact, all but four can be identified on the Palomar Sky Survey. In short, there are too few objects like 0202+14 in the 0.5-Jy sample for the obscuration hypothesis to be tenable. If, by some great fluke, all the objects without redshifts turned out to have $z \sim 3$–4, the fact that they are not very faint optically would indicate that the value $\tau^* = 0.1$ is a considerable overestimate; either way, dust obscuration does not seem important in this study.

We are left with the likelihood that the reduction in ϱ between $z \simeq 2$ and 4 is real; there are various ways in which this may be interpreted. First, it is often stated (e.g. Longair & Rees 1973) that the short lifetimes ($\sim 10^8$ yr) of powerful sources imply that changes with time in the RLF reflect directly the time variation of the source birth-rate. From this point of view, we would conclude that the rate of creation peaked at $z \simeq 2$. This statement is based on ignoring the first term in equation (2.1), and thus depends on the constancy of $\dot{P}$ ($\partial P/\partial t$ for an individual source) with cosmological epoch. The observed situation could thus be accounted for by having Q (the birthrate) constant and $\dot{P}$ increasing between $z = 2$ and 4, i.e. shorter source lifetimes at higher redshift. A further complication is that a galaxy with a given central powerhouse will produce a radio source with a different luminosity depending on its environment: a higher IGM density can mean a smaller source and hence a higher luminosity for a given energy output from the nucleus (e.g. Scheuer 1974). Since the powerful sources we are concerned with are not in rich clusters at

the present epoch (Longair & Seldner 1979), the relevant IGM density was probably higher at $z \simeq 4$ than at present. This would counteract any effect of a shorter lifetime and raise ρ at high redshift. Clearly, these effects need to be studied in detail, but, in practice, the range of redshifts involved is sufficiently small that we may indeed simply be observing an epoch of creation of galaxies with powerful central engines.

To make a connection with galaxy formation in general, we must realize that radio galaxies are peculiar first in being elliptical only and secondly in possessing a central engine. The latter point will cause radio sources to switch on some time later than any general epoch of galaxy formation; so too will the former if we believe ellipticals to have formed via mergers. No estimate of the delay can be given without great difficulty. We shall content ourselves here with noting that the observed changes in the RLF are occurring over quite long time-scales: for $H_0 = 50\,\mathrm{km\,s^{-1}\,Mpc^{-1}}$, the time elapsed between $z=2$ and 4 is 2.7×10^9 yr ($q_0=0$) or 1.4×10^9 yr ($q_0=0.5$). The important theoretical question is whether the turning-on of radio emission can take significantly longer than this. If it cannot, then the deficit of radio sources at high redshift reported here may indeed be directly connected with the formation of galaxies.

From this point of view, the recent infrared observations of radio galaxies at high redshift by Lilly & Longair (1984) and Lilly, Longair & Allington-Smith (1985) are of great interest, since measurement of the infrared-optical colour allows an estimate to be made of the time elapsed since the epoch of last major star-formation. The above authors find some galaxies at $z \simeq 2$ which show no evidence for recent star formation and which must have formed at $z \geqslant 4$. Conversely other galaxies found at $z \simeq 1$ are very blue ($r-K=3$–4) and these could have formed at $z \simeq 2$. This is certainly in accord with our ideas about galaxy formation: there must have been a range of protogalaxy collapse times, rather than a universal epoch of activity. The important question is whether the blue galaxies are truly young or simply having star formation triggered by some external interaction. Detailed studies of such objects will clearly have an important bearing on the interpretation of the redshift cut-off.

References

Allen, D. A., Wright, A. E. & Ables, J. G., 1982. *J. Astrophys. Astr.*, **3,** 189.

Allington-Smith, J. R., 1982. *Mon. Not. R. astr. Soc.*, **199,** 611.

Allington-Smith, J. R., 1984. *Mon. Not. R. astr. Soc.*, **209,** 665.

Allington-Smith, J. R., Perryman, M. A. C., Longair, M. S., Gunn, J. E. & Westphal, J. A., 1982. *Mon. Not. R. astr. Soc.*, **201,** 331.

Auriemma, C., Perola, G. C., Ekers, R., Fanti, R., Lari, C., Jaffe, W. & Ulrich, M.-H., 1977. *Astr. Astrophys.*, **57,** 41.

Avni, Y. & Bahcall, J. N., 1980. *Astrophys. J.*, **235,** 694.

Avni, Y. & Schiller, N., 1983. *Astrophys. J.*, **267,** 1.

Benn, C. R., 1981. *PhD thesis,* University of Cambridge.

Benn, C. R., Wall, J. V., Grueff, G. & Vigotti, M., 1984. *Mon. Not. R. astr. Soc.*, **209,** 683.

Bridle, A. H., Davis, M. M., Fomalont, E. B. & Lequeux, J., 1972. *Astr. J.*, **77,** 405.

Condon, J. J., 1984. *Astrophys. J.*, **287,** 461.

Condon, J. J. & Ledden, J. G., 1982. *Astr. J.*, **87,** 219.

Downes, A. J. B., Peacock, J. A., Savage, A. & Carrie, D. R., 1985. *Mon. Not. R. astr. Soc.*, in press.

Fanti, R., Gioia, I., Lari, C., Lequeux, J. & Lucas, R., 1973. *Astr. Astrophys.*, **24,** 69.

Fomalont, E. B., Kellermann, K. I., Wall, J. V. & Weistrop, D., 1984. *Science,* **225,** 23.

Gunn, J. E., Hoessel, J. G., Westphal, J. A., Perryman, M. A. C. & Longair, M. S., 1981. *Mon. Not. R. astr. Soc.*, **194,** 111.

Jenkins, C. R., 1982. *Mon. Not. R. astr. Soc.*, **200,** 705.

Kellermann, K. I. & Wall, J. V., 1983. *Early Evolution of the Universe and its Present Structure, IAU Symp. No. 104,* p. 81, Reidel, Dordrecht, Holland.

Koo, D. C., 1983. *Quasars and Gravitational Lenses, Proc. 24th Liège Symposium,* p. 240.

Kron, R. G., Koo, D. C. & Windhorst, R. A., 1985. *Astr. Astrophys.* **146,** 38.

Kühr, H., 1980. *PhD thesis,* University of Bonn.
Laing, R. A. & Peacock, J. A., 1980. *Mon. Not. R. astr. Soc.,* **190,** 903.
Laing, R. A., Riley, J. M. & Longair, M. S., 1983. *Mon. Not. R. astr. Soc.,* **204,** 151.
Lebofsky, M. J., Rieke, G. H. & Walsh, D., 1983. *Mon. Not. R. astr. Soc.,* **203,** 727.
Lilly, S. J. & Longair, M. S., 1984. *Mon. Not. R. astr. Soc.,* **211,** 833.
Lilly, S. J., Longair, M. S. & Allington-Smith, J. R., 1985. *Mon. Not. R. astr. Soc.,* **215,** 37.
Longair, M. S. & Rees, M. J., 1973. *Cargèse Lectures in Physics,* Vol. 6, Gordon & Breach.
Longair, M. S. & Seldner, M., 1979. *Mon. Not. R. astr. Soc.,* **189,** 433.
Machalski, J., 1981. *Astr. Astrophys. Suppl.,* **43,** 91.
Osmer, P. S., 1983. *Quasars and Gravitational Lenses, Proc. 14th Liège Symposium,* p. 51.
Osmer, P. S. & Smith, M. G., 1980. *Astrophys. J. Suppl.,* **42,** 333.
Ostriker, J. P. & Heisler, J., 1984. *Astrophys. J.,* **278,** 1.
Peacock, J. A., 1982. *Mon. Not. R. astr. Soc.,* **199,** 987.
Peacock, J. A., 1983. *Mon. Not. R. astr. Soc.,* **202,** 615.
Peacock, J. A. & Gull, S. F., 1981. *Mon. Not. R. astr. Soc.,* **196,** 611.
Peacock, J. A. & Wall, J. V., 1981. *Mon. Not. R. astr. Soc.,* **194,** 331.
Peacock, J. A. & Wall, J. V., 1982. *Mon. Not. R. astr. Soc.,* **198,** 834.
Peacock, J. A., Perryman, M. A. C., Longair, M. S., Gunn, J. E. & Westphal, J. A., 1981. *Mon. Not. R. astr. Soc.,* **194,** 601.
Pfleiderer, J., 1973. *Mitt. Astr. G.,* **32,** 108.
Rieke, G. H., Lebofsky, M. J. & Wisniewski, W. Z., 1982. *Astrophys. J.,* **263,** 73.
Savage, A. & Peterson, B. A., 1983. *Early Evolution of the Universe and its Present Structure, IAU Symp. No. 104,* p. 57, Reidel, Dordrecht, Holland.
Scheuer, P. A. G., 1974. *Mon. Not. R. astr. Soc.,* **166,** 513.
Spinrad, H., Stauffer, J. & Butcher, H., 1981. *Astrophys. J.,* **244,** 382.
Swarup, G., Subrahmanya, C. R. & Kapahi, V. U., 1982. *Proc. Vatican Study Week, Astrophysical Cosmology,* Pont. Acad. Scient. Scripta Varia 48, p. 383.
van der Laan, H. & Windhorst, R. A., 1982. *Proc. Vatican Study Week, Astrophysical Cosmology,* Pont. Acad. Scient. Scripta Varia 48, p. 349.
Wall, J. V. & Peacock, J. A., 1985. *Mon. Not. R. astr. Soc.,* **216,** 173.
Wall, J. V., Pearson, T. J. & Longair, M. S., 1980. *Mon. Not. R. astr. Soc.,* **198,** 683.
Wall, J. V., Pearson, T. J. & Longair, M. S., 1981. *Mon. Not. R. astr. Soc.,* **196,** 597.
Wills, D. & Lynds, R., 1978. *Astrophys. J. Suppl.,* **36,** 317.
Windhorst, R. A., 1984. *PhD thesis,* University of Leiden.
Wright, A. E., Jauncey, J. L., Bolton, J. G. & Savage, A., 1982. *Aust. J. Phys.,* **35,** 177.

Appendix 1: Practical aspects of model building

A1.1 RADIO SPECTRA AND SELECTION EFFECTS

The first problem encountered when integrating a trial luminosity function is that not all objects have the same spectrum. The possible responses to this range from the assumption of a single spectral index for all sources (e.g. WPLI) to attempts to model the distribution of spectral indices in detail (e.g. Machalski 1981; Condon 1984). The question is really one of how much detail is necessary to answer the important questions about the evolution of the RLF. If we wish to find the value of $\varrho(P,z)$ precisely, then errors in spectral index can be important, as may be seen by considering the cosmological inverse-square law:

$$S=\frac{P}{D^2(1+z)^{3+\alpha}}, \tag{A1.1}$$

where S is flux density, P luminosity, D angular diameter distance and α spectral index in the sense $S\propto\nu^{-\alpha}$. For a given S and α, an error in α alters P and thus ϱ; since ϱ is a fast-changing function of P, small errors in α can change ϱ considerably at high z. Consider first the situation where all sources have the same spectral index, α. If a different, incorrect, value of α is assumed in

constructing the P–z plane, then (A1.1) shows that our calculated luminosities will be in error due to the radio K-correction:

$$P' = P(1+z)^{\Delta\alpha}. \tag{A1.2}$$

In principle, this could be important. Suppose the true RLF is $\varrho_0 \propto P^{-\gamma}$ with no evolution; the systematic error in P then produces apparent evolution in the derived RLF:

$$\varrho'(P') = \varrho_0(P')(1+z)^{\gamma\Delta\alpha}. \tag{A1.3}$$

As the relevant values of γ can be in excess of 2 at high luminosities (Wall & Peacock 1985), it is important to keep $\Delta\alpha$ small. At $z=1$, $\Delta\alpha=0.2$ corresponds to an error of about 0.2 in $\log_{10}(\varrho)$, which is probably the maximum acceptable given the uncertainty in ϱ. At higher z, the uncertainty in ϱ increases faster than the error (A1.3) – see Section 4. We may be confident that $\langle\alpha\rangle$ has been chosen sufficiently accurately that these systematic errors are not important.

For flat-spectrum sources especially, there is also the worry that non-linear effects of the above kind may enter, not through errors in $\langle\alpha\rangle$ but due to the large spread of spectral indices. From a given set of (S, z) data, we will derive a different RLF ϱ_α for a given assumed spectral index. If we integrate ϱ_α over a distribution of α to find the mean value of ϱ, there is a systematic effect analogous to the classical Malmquist bias:

$$\langle\varrho\rangle = \varrho_\alpha(\langle\alpha\rangle) + \frac{d^2\varrho_\alpha}{d\alpha^2}\frac{\sigma_\alpha^2}{2}. \tag{A1.4}$$

Now, ϱ is related to a fixed $dN(S,z)$ by

$$dN(S,z) = \varrho(P,z)\frac{dV}{dz}\frac{A}{4\pi}d\log_{10}S\,dz, \tag{A1.5}$$

where V is comoving volume and A area in steradians. Hence, using (A1.1),

$$\frac{d^2\varrho_\alpha}{d\alpha^2} = \{\log(1+z)\}^2\frac{d^2\varrho}{d(\log P)^2} \tag{A1.6}$$

so that, if locally $\varrho \propto P^{-\gamma}$, we have

$$\frac{\Delta\varrho}{\varrho} = \tfrac{1}{2}\gamma^2\sigma_\alpha^2\ln^2(1+z). \tag{A1.7}$$

Taking typical figures for the most interesting areas of the flat-spectrum P–z plane ($z=1$, $\gamma=2.5$, $\sigma=0.3$), the correction is again acceptably small (about 0.1 in $\log_{10}\varrho$); this would not have been so with $\gamma \geqslant 5$. It is interesting to note that Condon (1984) carried out a similar analysis, but with the opposite conclusion. This was because he considered the error in $dN(S,z)$ for a fixed ϱ; errors of even few per cent are then statistically significant. Our point of view is that it is preferable to regard the errors as attaching to ϱ, as this is what we are attempting to deduce.

Thus, as far as finding the RLF is concerned, the only feature of spectral index distributions which needs to be considered is the division into two populations, namely steep-spectrum and flat-spectrum sources. This classification has been adopted by all authors who have analysed high-frequency survey data, and may be looked at in several ways. First, it is a practical method of dealing with objects where spectral indices can range from +1 to −1 – too wide a dispersion to be modelled as a single-α population (see above). More physically, it is well established that flat-spectrum objects have emission dominated by a compact, self-absorbed component at centimetre wavelengths. The dividing criterion is usually set at $\alpha=0.5$ (where α is measured at

high frequencies e.g. $\alpha_{2.7\,\mathrm{GHz}}^{5\,\mathrm{GHz}}$ in this paper), since sources with optically thin synchrotron emission invariably have spectra steeper than this. Objections to this scheme hinge on the fact that it is imprecise: at sufficiently high frequencies, all objects could be optically thin. Nevertheless, the structures of flat-spectrum sources do differ from those with steep spectra; since the majority of data relevant to RLF estimation exist in surveys at ~1 GHz, it is justifiable to use an empirical criterion based on the high-frequency spectrum as an indicator of this physical distinction. What we must recognize is that our modelling will be valid only over a restricted range of frequencies set by the scale of spectral curvature. In particular, as discovered by PG, 178 MHz is too remote from 2.7 GHz, and 3CR data are thus not considered in this paper.

A related criticism is that by Savage & Peterson (1983) concerning redshift effects: as flat-spectrum sources are placed at higher redshifts, the rest-frame frequency rises and they will eventually be classified as steep-spectrum. Whether this effect is important can be investigated by using the complete 2.7-GHz sample of Peacock & Wall (1981) as amended by Wall & Peacock (1985). This contains 171 sources with $S_{2.7}>1.5$ Jy, for very nearly all of which we have flux densities at 1.4, 2.7, 5 and 10.6 or 15 GHz. These had previously been classified as steep- or flat-spectrum using $\alpha_{2.7}^{5}$; if we repeat the analysis using $\alpha_{1.4}^{2.7}$ and $\alpha_{5}^{10.6}$, this simulates moving the sources over the redshift range 0 to 4, since most flat-spectrum sources in the sample have $z\simeq1$. The original diversion of the sample was 120/51 steep/flat and the two alternative spectral criteria give 117/54 and 122/49 respectively. This demonstrates that the scale of spectral curvature in most flat-spectrum sources is sufficiently broad that the effect postulated by Savage & Peterson (1983) will probably not become significant unless redshifts $\geqslant10$ are considered. This point is considered in more detail in Section 4.4.

To summarize, the dual-population model adopted by WPLII, PG and others still provides a suitable basis for estimating the RLF. The simplification of neglecting a spread in spectral index produces no important error in the derived space densities.

A1.2 THE P–α RELATION

The incorporation of the known correlation between spectral index and luminosity was important to the PG analysis, since it allowed samples defined at different frequencies to be used in a single framework. Adopting a single value of α would not have been satisfactory, since the various data sets are not simply related by a shift in flux density. However, the form adopted for the mean P–α relation by PG needs to be modified. PG used the results of Laing & Peacock (1980), who investigated the P–α relation for extended sources. In fact, a large proportion (~25 per cent) of the steep-spectrum sources found in samples selected at high frequencies surprisingly turned out to have compact structures similar to flat-spectrum sources (see e.g. Peacock & Wall 1982). The addition of these objects makes the P–α relation for steep-spectrum sources in the amended 1.5-Jy sample of Peacock & Wall (1981) considerably less strong. Fig. A1 shows the P–α plot for this sample; the correlation is much weaker than assumed by PG. For example, the most luminous sources [with $\log_{10}(P_{2.7}\,\mathrm{W\,Hz^{-1}\,sr^{-1}})>26$] have a mean spectral index $\langle\alpha\rangle=0.83$ and an RMS dispersion $\sigma_\alpha=0.18$ – not much of an increase over the value $\alpha=0.75$ assumed by PG for the weakest sources. In fact, Malmquist-like selection effects reduce $\langle\alpha\rangle$ in a flux-density-limited sample and may be analysed as follows.

Assume that at a given point on the P–z plane, we have a distribution of spectral indices $f(\alpha)$, with mean $\bar{\alpha}$. This is not the mean observed in a flux-density-limited sample: at a given α, the number of objects seen is $f(\alpha)N(\alpha)d\alpha$, where $N(\alpha)$ is the number that would be observed if all sources had the same spectral index. Thus, as proved by PG, there is a bias in $\langle\alpha\rangle$:

$$\langle\alpha-\bar{\alpha}\rangle=k\sigma_\alpha^2 \qquad \text{(A1.8)}$$

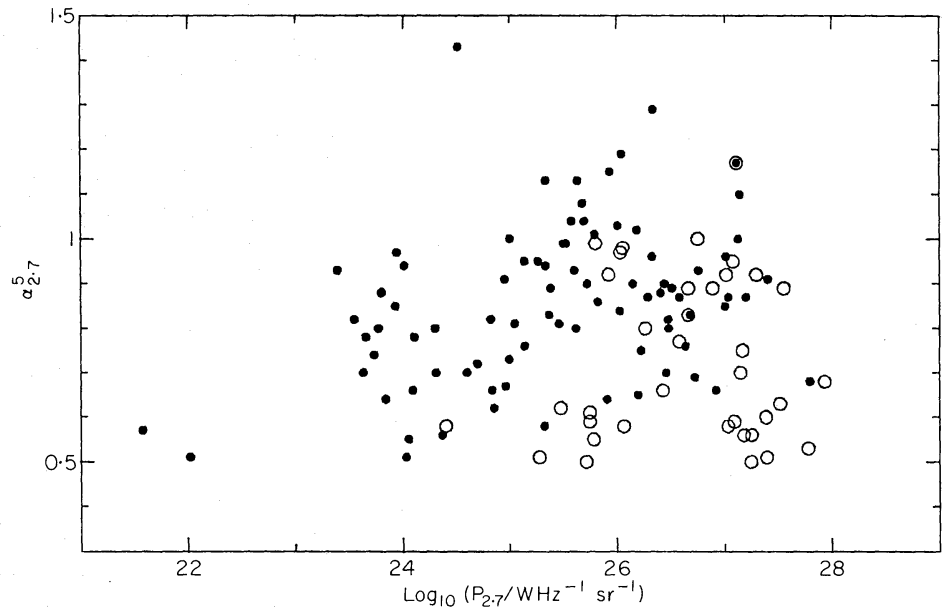

Figure A1. The P–α relation for steep-spectrum sources in the 1.5-Jy sample of Peacock & Wall (1981). (q_0=0.5 has been assumed.) Open circles denote compact sources (unresolved with the Cambridge 5-km Telescope).

where

$$k=\frac{1}{N(\alpha)}\frac{dN(\alpha)}{d\alpha}. \tag{A1.9}$$

We are interested in finding k for a sample restricted also in luminosity (i.e. $\Delta\alpha$ as a function of P). This was done numerically by PG, but the following argument is more transparent. Suppose we have $\varrho(P,z)\propto V(z)^{\delta}$ near the sample limit [$V(z)$ is the cosmological volume enclosed by redshift z and depends on α for fixed P and S – see equation A1.1]; δ simply represents the change of ϱ with z. In this case, as $N=\int\varrho dV$, we have

$$k=\frac{\delta+1}{V}\frac{dV}{d\alpha}. \tag{A1.10}$$

Given $V(z)$ and $z(\alpha)$ via (A1.1), we can find k.

For q_0=0.5, the result is

$$k=\frac{3(\delta+1)}{2}\frac{\ln(1+z)}{1+(1+\bar{\alpha})(\sqrt{1+z}-1)}. \tag{A1.11}$$

Now, we can find β once we know $\langle V/V_{\max}\rangle$ for the sample under consideration, as $\langle V/V_{\max}\rangle=(\delta+1)/(\delta+2)$. Peacock *et al.* (1981) give $\langle V/V_{\max}\rangle=0.661\pm0.036$ for steep-spectrum sources with $P<10^{26}\,\mathrm{W\,Hz^{-1}\,sr^{-1}}$, implying that $\delta=1$ within the errors (in fact Peacock *et al.* assumed $q_0=0$, but this does not alter δ significantly). For the powerful sources, $z\sim1$ and k is a slow function of z (and thus P). We adopted the typical value for $\delta=1$, $z=1$, $\bar{\alpha}=0.8$ of $k=1.2$. Finally, therefore, with $\sigma_\alpha=0.18$, the true mean spectral index of the powerful sources in the 1.5-Jy sample is 0.87.

Given the scatter, the precise expression chosen to represent the variation of $\langle\alpha\rangle$ with P is not important. The form used by PG is slightly against the spirit of this investigation, since it has a discontinuous first derivative. Instead, the following expression was adopted:

$$\begin{aligned}&\alpha=0.75 && P_{2.7}<10^{24}\,\mathrm{W\,Hz^{-1}\,sr^{-1}}\\ &\alpha=0.75+0.015\,(\log_{10}P-24)^2 && P_{2.7}>10^{24}\,\mathrm{W\,Hz^{-1}\,sr^{-1}}.\end{aligned} \tag{A1.12}$$

This is *ad hoc*, but it represents the rise to higher α in a satisfactory way; the only important change from PG is that high-luminosity sources have less steep spectra by about $\Delta\alpha=0.1$ than previously assumed.

Finally, for the flat-spectrum sources, there is no reason to alter PG's assumption of $\langle\alpha\rangle=0$, independent of luminosity. This approach is crude in comparison with the care devoted to obtaining the correct $\langle\alpha\rangle$ for steep-spectrum sources, but we emphasize that such attention to detail is needed only to relate data at different frequencies, *not* to obtain correct space densities.

A1.3 INTEGRATION SCHEMES

In principle, integration of the RLF to find the number of objects selected by constraints in redshift, luminosity, flux density, etc. is straightforward, but in practice difficulties are introduced because $\varrho(P,z)$ is a fast-changing function.

This caused problems with the results of PG; exact integration of their RLFs yields results sometimes in error by ~30 per cent with respect to observation (de Zotti, Lawrence; private communications). In retrospect, this is not surprising given the method of integration, which was the same as that used by WPL: the P–z plane was divided into a grid of 100×100 cells and the contribution to the integrand of a given cell counted only when the centre of the cell lay within the area of integration. Since the single-cell contribution was taken as proportional to the value of $\varrho(P,z)$ at the cell centre, this scheme runs into problems with fast-changing forms for ϱ, as the assumption is that ϱ is constant over the cell (width 0.1 in $\log_{10}P$). This does not invalidate the results of PG, since the effect of the integration errors is only to distort the P–z plane by small fractions of a cell size – the large-scale features in ϱ are preserved. Nevertheless, the fact that the PG RLFs cannot be integrated directly is clearly a disadvantage.

The present work therefore uses a scheme with interpolation within a cell to estimate the individual contributions to the integral more accurately. This reduced the integration error to less than ~2 per cent while allowing a coarser grid of 50×50 points to be used. The grid covered the range $P_{2.7}=10^{20}$ to $10^{30}\,\mathrm{W\,Hz^{-1}\,sr^{-1}}$ linearly in $\log P$ and the range $z=0.01$ to 10 linearly in $\log z$. Note that PG extended the integration to $z=100$, but the possible contributions from these extreme redshifts are so uncertain that it was considered pointless to retain them. Also, since the present work considers fainter surveys than PG, it was necessary to include objects of lower luminosity than $10^{20}\,\mathrm{W\,Hz^{-1}\,sr^{-1}}$; as these enter only at low redshift, the contribution between $P_{2.7}=10^{18}$ and $10^{20}\,\mathrm{W\,Hz^{-1}\,sr^{-1}}$ was added as a separate one-dimensional integration – assuming no evolution in ϱ.

Appendix 2: Data

A2.1 S–z DISTRIBUTIONS

Radio samples with anything approaching complete redshift information are rare. Only two have been published: the 178-MHz sample of Laing, Riley & Longair (1983) and the 2.7-GHz sample of Peacock & Wall (1981). These samples have many sources in common, which is fortunate since Appendix 1 has established that spectral curvature makes it impossible to work with frequencies as low as 178 MHz within the present framework. The Peacock & Wall sample contains 168 sources with $S_{2.7}>1.5$ Jy in the Northern Hemisphere; this has been extended to the whole extragalactic sky by Wall & Peacock (1985), producing a sample of 233 sources with $S_{2.7}>2$ Jy. There is some overlap with the earlier work, leaving an independent sample of 80 sources with $S_{2.7}$ in the range 1.5–2 Jy.

The principal reason for uncertainty in the RLF is the lack of fainter samples with extensive redshift data. An important recent piece of work was thus the resurvey of the Parkes $\pm4°$ zone

Table A1. The 0.5-Jy sample.

Source	$S_{2.7}$/Jy	$\alpha_{2.7}^{5}$	ID	m	z
0013-005	0.80	0.34	Q?	19.5	1.928*
0038-020	0.72	0.41	Q	18.5	1.176
0111+021	0.63	-0.05	G	16.3	0.047
0112-017	0.94	-0.26	Q	18.0	1.365
0115-016	0.64	0.22	EF		1.000*
0122-003	1.19	-0.13	Q	17.0	1.085
0213-026	0.54	-0.58	EF		1.000*
0215+015	0.73	-0.61	Q	18.5	1.135*
0216+011	0.62	-0.27	Q	20.0	2.512*
0226-038	0.77	0.13	Q	17.5	2.064
0237-027	0.68	-0.87	Q	19.0	1.116
0421+019	0.83	0.21	Q	17.5	2.048
0422+004	1.28	-0.36	Q	16.0	0.302*
0440-003	1.85	0.45	Q	19.2	0.850
0458-020	1.89	-0.24	Q	20.0	2.286
0823+033	1.03	0.15	Q?	18.5	1.135*
0837+035	0.69	0.28	Q?	20.0	2.512*
0906+015	0.97	-0.35	Q	18.0	1.018
0907-023	0.52	0.43	Q	18.0	0.957
0922+005	0.82	0.26	Q	18.5	1.720
1004-018	0.59	0.17	Q	19.2	1.212
1008-017	0.95	0.41	G?	19.4	0.380*
1103-006	0.59	0.48	Q	15.4	0.427
1217+023	0.51	0.24	Q	16.5	0.240
1218-024	0.57	0.42	Q	19.0	1.479*
1222+037	1.08	0.09	Q	18.8	0.957
1229-021	1.19	0.45	Q	16.8	1.041
1302-034	0.60	0.17	Q	19.4	1.250
1317+019	0.59	0.00	G?	19.5	0.398*
1351-018	0.80	-0.04	Q?	21.0	4.266*
1356+022	0.75	0.16	Q	18.3	1.329
1402-012	0.73	0.32	Q	18.2	2.518
2012-017	0.78	0.35	Q	17.5	0.668*
2047+039	0.57	-0.16	Q	18.5	1.135*
2059+034	0.50	0.14	Q	18.0	1.013
2215+020	0.65	0.05	G?	21.5	0.871*
2224+006	0.52	0.10	G?	21.8	1.148*
2245+029	0.73	0.29	Q?	20.0	2.512*
2320-035	0.89	0.17	Q	18.6	1.410
2332-017	0.56	-0.03	Q	18.5	1.185
2335-027	0.63	0.11	Q	19.2	1.072

described by Wright *et al.* (1982): from this it proved possible to select a sample of 41 flat-spectrum sources having $2>S_{2.7}>0.5$ Jy, of which only four lacked optical identifications (subsequently, CCD identifications were obtained for 2215+020 and 2224+006; Wall *et al.*, in preparation). These sources were selected from an area of 0.584 sr, produced by neglecting RAs of 5^h–8^h and 15^h–20^h, which are affected by obscuration associated with the Galactic plane. The sample is listed in Table A1; redshifts indicated by an asterisk have been estimated using the m–z relations for the 2-Jy sample described by Wall & Peacock. The two empty-field sources have been assigned redshifts of 1.

Table A2. 2.7-GHz complete samples.

Flux-density range	Area	N	No with uncertain z	No without ID	Spectral type
>2 Jy	9.81sr	165	31	5	Steep-Spectrum
		68	13	1	Flat-Spectrum
1.5-2 Jy	4.05sr	52	8	1	Steep-Spectrum
		28	9	0	Flat-Spectrum
0.5-2 Jy	0.584sr	41	16	2	Flat-Spectrum
		354	77	9	

The above three complete samples form the most important part of the data base used here, so it is vital to assess their reliability. Table A2 lists important parameters for the samples, in particular how many objects lack optical data. Overall, we have 354 sources, of which only 3 per cent are unidentified, and a further 19 per cent are identified but lack either a measured redshift or a secure estimate from galaxy photometry (a technique well-verified by recent redshifts in excess of 1 obtained for faint 3CR galaxies by e.g. Spinrad, Stauffer & Butcher 1981). These uncertain objects are either quasar candidates, objects too faint to be securely classified as galaxies, or simply empty fields. Wall & Peacock (1985) considered estimation of quasar redshifts from m–z relations and concluded that this could be carried out to within a factor 2. They also argued that the majority of faint identifications are likely to be galaxies, as found in deep investigations (e.g. Gunn *et al.* 1981). From our point of view, the greatest worry is the objects which could have very high redshifts: the fainter quasar candidates and the empty fields. There are 16 quasar candidates with $V>18$ and nine empty fields. For the latter, we have reason to believe the optical counterpart not to be very faint:

(i) Five of the nine have not been examined beyond the limit of sky survey plates. Those that have escaped detection with CCDs are usually short exposures, reaching only $R\simeq22.5$.

(ii) Some of the sources with no optical counterpart even in these deep searches have been detected in the infrared (0316+16: Allen, Wright & Ables 1982; 1624+41: Lebofsky, Rieke & Walsh 1983), suggesting that they lie not far below the present optical limit.

Redshifts are estimated for the unidentified objects on the assumption that they are galaxies at $\sim$1 mag below the relevant plate limit. Even if the redshifts of these objects were all very much higher than assumed, this need not change our data set statistically: out of 354 sources, we would need to take 25 to very high redshifts before the Kolmogorov–Smirnov test would detect a difference in the redshift distributions at the 5 per cent level.

We conclude that the incompleteness of the redshift data in the complete samples should be unimportant within the limits set by finite sample size. Section 4.4 discusses the effect of these unknown redshifts in more detail.

A2.2 IDENTIFICATION DATA

In addition to the above samples, there have been many attempts to identify sources selected at lower flux densities, but none have attained the completeness levels of the bright samples. Furthermore, these investigations contain essentially no redshift information. Nevertheless, in the absence of perfect data, something may be learned from partial identification results. As for the bright samples, the basic method is redshift estimation from apparent magnitude. While this is

legitimate in approximating a few missing redshifts, the application of the 'standard candle' hypothesis to a whole sample is clearly dangerous. Disregarding possible errors in image classification (galaxy/stellar) and in magnitude scales, there is the uncertainty introduced by the galaxy bivariate luminosity function. This tells us that there is a positive correlation between radio and optical luminosities: below the break in the RLF at $P_{2.7}\sim10^{24}$ W Hz^{-1} sr^{-1} radio galaxies have less bright absolute magnitudes than do the most powerful radio galaxies (see e.g. Auriemma *et al.* 1977; Swarup *et al.* 1982). We can estimate roughly at what point this becomes important: consider a survey down to a flux density $S_{\rm LIM}$, for which galaxy identifications are available to a magnitude $m_{\rm LIM}$, corresponding to a redshift $z_{\rm LIM}$ on the standard candle hypothesis. The typical luminosity of the identifications is given roughly from flux density $S_{\rm LIM}$ at $z_{\rm LIM}$; if this is above the break luminosity, then the standard candle hypothesis is self-consistent.

Typical values of $z_{\rm LIM}$ for deep plate material are ~1, which implies a critical flux-density limit of ~10 mJy at 408 MHz. Objects at this level which are identified thus cannot be of high luminosity – we expect the associated galaxies to be optically fainter and the assumed redshift limit should be modified. That this is an important effect is confirmed by the example of the Leiden–Berkeley Deep Survey (van der Laan & Windhorst 1982; Windhorst 1984; Kron, Koo & Windhorst 1985). With a radio limit of 0.6 mJy at 1.4 GHz, it should be subject to the above effect, although redshifts were estimated initially assuming that galaxies had the same absolute magnitude as 3CR. When some redshifts were eventually measured, it was indeed found that the galaxies were typically $\gtrsim1$ mag less luminous than had been assumed (this is partly due to the emergence of a new class of optical identification – see below).

The above uncertainties may nevertheless not have a critical effect on conclusions drawn from identification data. In this paper, we shall attempt to estimate one statistic only for these faint samples, namely the fraction of sources lying within a redshift z_0. This is obtained essentially from the fraction of sources identified with galaxies, relating the plate limit to z_0 via the standard candle hypothesis, bearing in mind the above discussion. In the samples used here, the fraction of stellar identifications is generally small and the assumption that these are quasars with $z>z_0$ does not greatly affect the result. The uncertainties in this procedure reduce to a question of the value of z_0: how accurate is it, and how accurate does it need to be? The dominant uncertainty lies in the value of absolute magnitude assumed for redshift estimation: if we assume we can predict this to within $\Delta\langle M\rangle=\pm0.5$ mag, the corresponding uncertainty is a factor of ~1.3 in z_0 (e.g. if we estimate $z_0=0.8$, it probably lies in the range 0.6–1.0). The effect this has on $f(z<z_0)$ is not large, because redshifts are distributed over a wide logarithmic range. For example, changing z_0 over the range 0.6–1.0 for the 2-Jy sample alters $f(z<z_0)$ by only ±9 per cent, even though this is at the peak of the redshift distribution, where f changes fastest. Since most of the faint samples considered here are small, the statistical errors on f are of this order anyway. If we have n sources out of N with $z<z_0$, the maximum-likelihood estimate for $f(z<z_0)\pm\sigma_f$ is [for $n(N-n)\gg N$],

$$f=\frac{n}{N}\pm\left\{\frac{n(N-n)}{N^3}\right\}^{1/2}. \qquad \text{(A2.1)}$$

We shall use the data from five faint samples drawn from four studies; these are summarized in Table A3, together with the adopted values of f. The samples were taken from:

(i) The B2 1-Jy sample described by Allington-Smith (1982) and Allington-Smith *et al.* (1982). This is based on CCD data and is the deepest of the faint samples.

Approximately 80 per cent of the sources are identified, galaxies and stellar objects accounting for 60 and 20 per cent respectively. Allington-Smith (1984) estimates redshifts for this sample using 3CR m–z relations; this should be accurate out to $z\simeq1$, beyond which the uncertain

Table A3. Estimated redshift distributions.

Frequency	Flux-density range	Spectral type	N	z_o	$f(z<z_o)$
408 MHz	1-2 Jy	All	59	1.25	0.51 ± 0.07
408 MHz	0.1-1 Jy	Steep-Spectrum	83	0.8	0.20 ± 0.04
408 MHz	0.01-0.1 Jy	Steep-Spectrum	60	0.5	0.22 ± 0.05
5 GHz	0.015-0.1 Jy	Flat-Spectrum	35	0.6	0.46 ± 0.08
1.4 GHz	>0.58 mJy	All	302	0.5	0.43 ± 0.03

contribution from quasar candidates dominates. We shall take 30 out of 59 sources to have $z<1.25$.

(ii) The 5C12 survey described by Benn (1981) (see also Benn *et al.* 1984 and references therein). For this, optical identifications were carried out on deep Palomar Schmidt plates reaching $R\simeq20.5$ and $B\simeq22.5$. Benn discusses redshift estimation from the 3CR m–z relation and concludes that his investigation has a limiting redshift of $z=0.8$. He defines two statistical 408-MHz samples at 10 and 100 mJy, for which 22 and 20 per cent respectively are identified with galaxies (after allowance for background contamination due to the low accuracy of the 5C position). Following the discussion on the bivariate luminosity function, we shall assume a 1-mag shift in absolute magnitude for the fainter sample, corresponding to a revised limiting redshift of 0.5.

(iii) Condon & Ledden (1982) report optical identifications on prints of the Palomar Sky Survey for a survey complete to 15 mJy at 4755 MHz. For their complete sample of 186 sources as a whole, they find only 55 identifications using accurate VLA positions. For the 39 flat-spectrum sources with $15\leqslant S<100$ mJy, on the other hand, they find 16 galaxies and five quasar candidates. Furthermore, identifications were not sought for three sources and a fourth was obscured by a bright star. We may therefore assume that 16 out of 35 sources have $z<0.6$ – the galaxy redshift corresponding to the PSS limit. Admittedly, the data on absolute magnitudes of flat-spectrum galaxies are poor in comparison with those which exist for steep-spectrum sources; we do not know if there is a similar correlation of optical and radio luminosity. For this small data set, however, the uncertainties in $f(z<z_0)$ are large and a 1-mag change in $\langle M\rangle$ from that appropriate to luminous flat-spectrum sources would not be important.

(iv) Finally, there is the Leiden–Berkeley deep survey discussed above. The most recent results of this massive project are given in the thesis by Windhorst (1984). The complete sample consists of 302 sources with $S>0.58$ mJy at 1.4 GHz, in an area of 1.68 msr. Identifications have been performed on Kitt Peak 4-m plates; allowing for contamination by unrelated background objects, the fraction of the sample identified with galaxies above the optical limits is 43 per cent. Plates were taken in four colours, the deepest reaching limiting magnitudes of 23 in F(6100 Å) and 24 in J(4650 Å). Assumption of a 3CR absolute magnitude would imply $z_0=0.8$–0.9, but, as for 5C, we may expect that a value of $z_0=0.5$ will be nearer the mark. This can be checked by comparison with the redshift data discussed by Windhorst (1984). Windhorst divides galaxies into two classes based on J–F colour and shows that the redder set have absolute magnitudes close to the standard giant elliptical value, whereas the blue galaxies are 1–2 mag fainter. Since the optical limit is a function of colour (only identifications appearing in both J and F were accepted), the limiting redshift for both classes appears close to 0.5 from the existing spectroscopy (32 objects).

To sum up, we have argued that the above estimates of $f(z<z_0)$ are unlikely to be systematically in error by more than their associated statistical errors. In fact, we may take the

Table A4. Source counts.

Frequency	Flux-density range	Spectral	Separation?	References
408 MHz	> 12 mJy		No	PG and refs therein
1.4 GHz	> 0.5 Jy		No	Bridle et al. (1972)
1.4 GHz	0.6 - 500 mJy		No	van der Laan & Windhorst (1982)
2.7 GHz	>0.1 Jy		Yes	Wall et al. (1981)
5.0 GHz	>0.015 Jy		Yes	Kühr (1980); Condon & Ledden (1982)
5.0 GHz	> 0.07 mJy		Yes	Kellermann & Wall (1983); Fomalont et al. (1984)

view that the existence of larger errors would not be disastrous for the RLF estimation based on these data sets. Without the above information, the redshifts of faint radio sources would be very uncertain; it is clear from PG that a solution would be possible in which all sources had $z\sim10$. It is important, then, to use the identification data to rule out such obviously incorrect possibilities. Even if f turned out to be grossly in error (say, by a factor of 1.5), this only affects our estimate of ϱ by a similar factor in the regions of the P–z plane covered by these data sets: we shall see that the uncertainty in the P–z plane is rarely smaller than this. In short, because we are interested in interpreting $\log(\varrho)$, uncertainties in $f(z<z_0)$ should be unimportant unless they approach a factor of 10; this is most unlikely.

A2.3 SOURCE COUNTS

Since the writing of PG, the source-count data at very low flux densities have been greatly extended, reaching to well below 1 mJy. Otherwise, the data sets used here are essentially those used by PG; Table A4 summarizes the available information. Note that the counts for many of the faint surveys are published only in diagrammatic form, but, in view of the large errors in this regime, inaccuracies in reading values for $dN(S)$ should not matter. Of especial importance is the extension of spectral index data to the lowest levels. Interestingly, once both steep- and flat-spectrum counts have turned over (below $S_{2.7}\simeq0.1$ Jy), they remain in a roughly constant ratio (of about 3 : 1) over three decades of flux density down to <1 mJy (see Fomalont *et al.* 1984; note that because of the small numbers involved, their faint counts have been merged into a single bin over the range 0.06–3 mJy.

A2.4 THE LOCAL RLF

The direct determinations of the low-luminosity end of the RLF used by PG still stand. Because of the extension to lower flux densities of the present work, however, it is necessary to extend the local RLF data to consider lower luminosities. The only major study of the local RLF for $P_{2.7}<10^{20}\,\mathrm{W\,Hz^{-1}\,sr^{-1}}$ is that by Pfleiderer (1973). His estimate of the local RLF in this range of luminosities is affected by an uncertain correction for incompleteness, which is stated to introduce a factor of 50 uncertainty. Error bars have been placed on ϱ by assuming that the

Table A5. RLF expansion coefficients.

order of term		Steep-Spectrum				
x	y	RLF 1	RLF 2	RLF 3	RLF 4	RLF 5
0	0	-2.16	-2.09	-2.06	-2.20	-2.08
1	0	-3.21	-4.49	-6.68	-4.35	-6.68
0	1	2.38	-4.29	-2.36	11.98	-6.08
2	0	-24.30	-21.38	-9.01	-19.52	-0.69
1	1	9.88	63.28	37.19	-111.41	42.75
0	2	202.26	197.98	21.47	139.74	191.92
3	0	-154.41	-129.89	-136.78	-107.94	-170.27
2	1	-213.21	-307.94	-238.63	241.91	-719.16
1	2	-579.46	-940.28	15.32	-469.86	911.78
0	3	-293.94	34.72	-15.59	-60.87	-1376.20
4	0	838.89	756.08	675.86	591.08	717.67
3	1	609.51	854.98	330.08	-64.28	2207.38
2	2	25.69	626.43	255.72	647.11	-4856.30
1	3	1874.53	1125.63	-258.71	-358.44	5628.31
0	4	-745.25	-671.15	38.81	298.44	-999.15
5	0	-1286.02	-1261.06	-1037.18	-912.17	-1088.17
4	1	-284.75	-638.92	49.29	42.73	-1628.39
3	2	70.93	148.64	-763.76	-956.22	4020.87
2	3	-1751.67	-1411.64	818.52	1691.21	-4460.82
1	4	1328.62	998.22	-342.26	-1348.21	935.06
0	5	-260.91	-103.90	75.13	339.64	80.72
6	0	608.35	675.83	482.07	437.24	548.12

order of term		Flat-Spectrum				
x	y	RLF 1	RLF 2	RLF 3	RLF 4	RLF 5
0	0	-3.51	-3.79	-3.67	-3.80	-3.59
1	0	-7.10	-8.02	-6.10	-7.46	-8.46
0	1	3.18	14.88	1.10	16.77	-0.59
2	0	-9.56	8.05	-5.62	5.51	-2.25
1	1	20.88	-27.17	-17.13	-28.72	22.10
0	2	-159.21	-345.42	2.55	-424.53	-42.22
3	0	12.16	-34.91	-10.08	-35.26	11.90
2	1	166.80	280.66	144.62	376.71	83.54
1	2	-127.12	197.80	-75.98	5.86	-259.76
0	3	249.82	400.88	-11.25	900.42	196.07
4	0	-9.64	25.22	13.75	30.41	-23.97
3	1	-223.66	-315.59	-185.23	-485.60	-51.06
2	2	351.43	244.08	198.88	867.15	138.20
1	3	-268.18	-454.26	-115.19	-1632.85	28.89
0	4	-10.67	-17.58	48.71	379.09	-100.05

quoted error corresponds to $\pm 2\sigma$. In this regime, the RLF is dominated by the contribution from spiral and irregular galaxies, which are found to be steep-spectrum only (see Fanti *et al.* 1973). The steep-spectrum local RLF was therefore determined directly from Pfleiderer's values after transformation to 2.7 GHz (assuming $\alpha = 0.75$). The overall data (plotted in Fig. 2) are in good agreement with the local RLF derived by Windhorst (1984).

A low-luminosity extension of the flat-spectrum RLF may be constructed from the study by Jenkins (1982). This was confined to E and S0 galaxies only, but the contribution of S and I galaxies to the flat-spectrum population appears to be small (see above). The flat-spectrum

component of the luminosity function derived by Jenkins is consistent with that used by PG in the region of overlap, but extends to a factor of 30 fainter. We are thus able to add an additional point to the four used by PG, establishing the flat-spectrum local RLF over four decades of luminosity. Interestingly, the data are consistent with a single power-law, of the form $\varrho \propto P^{-1}$.

The local RLF data have been subjected to a small (~10 per cent) correction to allow for binning in luminosity; when the bins are over a very large luminosity range, the value of ϱ at the bin centre can be overestimated.

The local RLF is used to fix the model value of $\varrho(P, z)$ at $z=0$. Since the work of the Leiden–Berkeley group discussed above has established that ϱ does not change significantly for $z<0.2$, the model RLFs in the present work were constrained also to be consistent with the local RLF at $z=0.2$.

Appendix 3: Model RLF parameters

We first define coordinates $x(P)$ and $y(z)$ and expand ϱ:

$$\log_{10}\varrho = \sum_{i=0}^{n}\sum_{j=0}^{n-i} A_{ij}x^i y^j.$$

In all cases, $x=0.1$ ($\log_{10}P-20$) was taken. For RLFs 1, 2, 4 and 5, $y=0.1z$, but $y=\log_{10}(1+z)$ for RLF 3. For RLF 2, we add an exponential luminosity cut-off:

$$\varrho \rightarrow \varrho \exp(-P/10^{28}).$$

All RLFs should be integrated over the range $P_{2.7}=10^{18}$–10^{30} W Hz^{-1} sr^{-1} and $z=0$–10 except RLF 3, which should be integrated over $z=0$–5. The coefficients A_{ij} are given in Table A5 and the spectral index assumptions in Section A1.2 of Appendix 1.